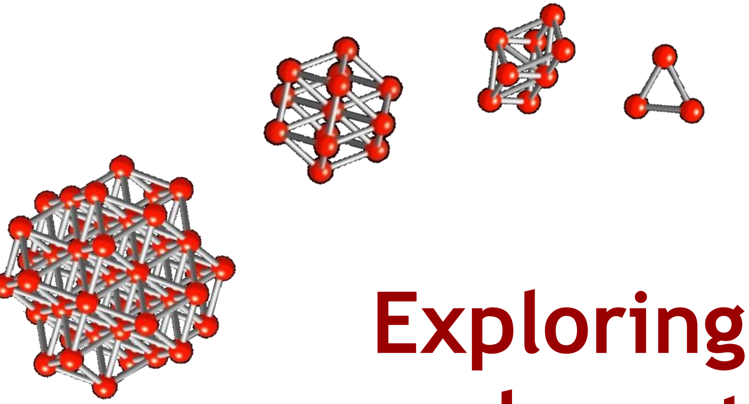

Exploring materials function and reactivity *in situ*

Karena W. Chapman

Endowed Chair in Materials Chemistry
Department of Chemistry, Stony Brook University

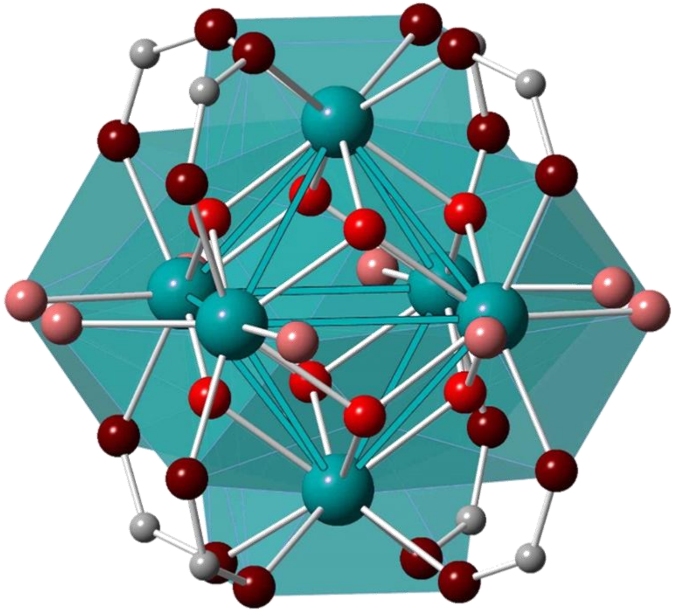

Stony Brook University

Clean energy research spanning many applications

Understanding function & reactivity from atoms to applications

Gas capture (e.g. CO_2)

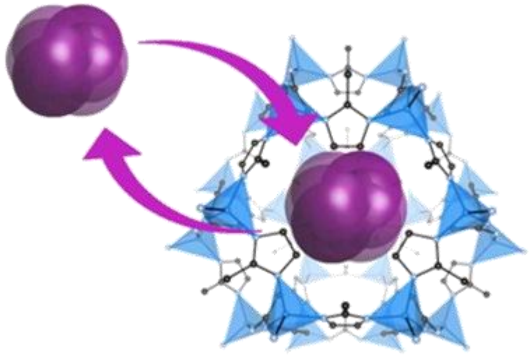

Designing Catalysts

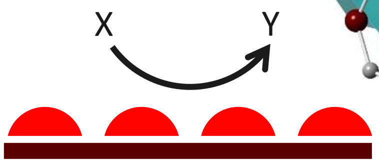

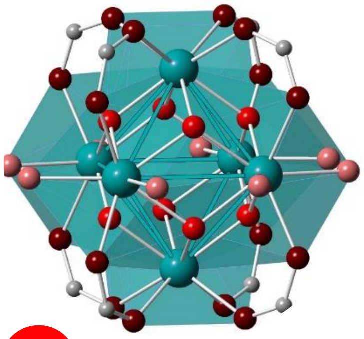

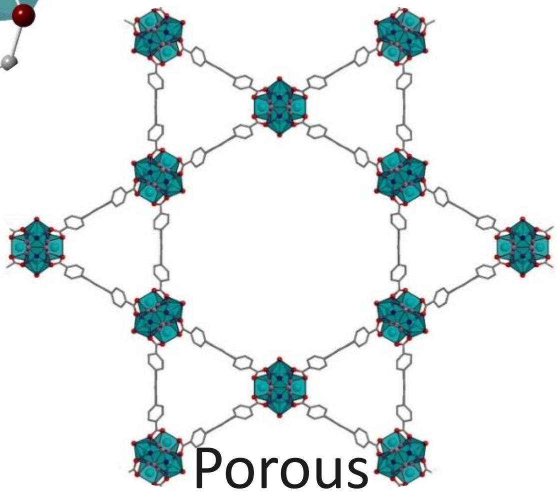

Porous Materials

Energy Storage

Science of Synthesis

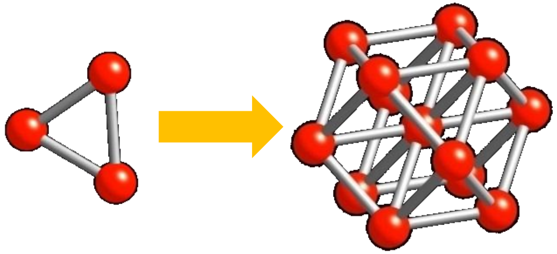

Illuminating structure, function & reactivity

X-rays can penetrate working
systems without damage,
to allow us to probe their function
and reactivity

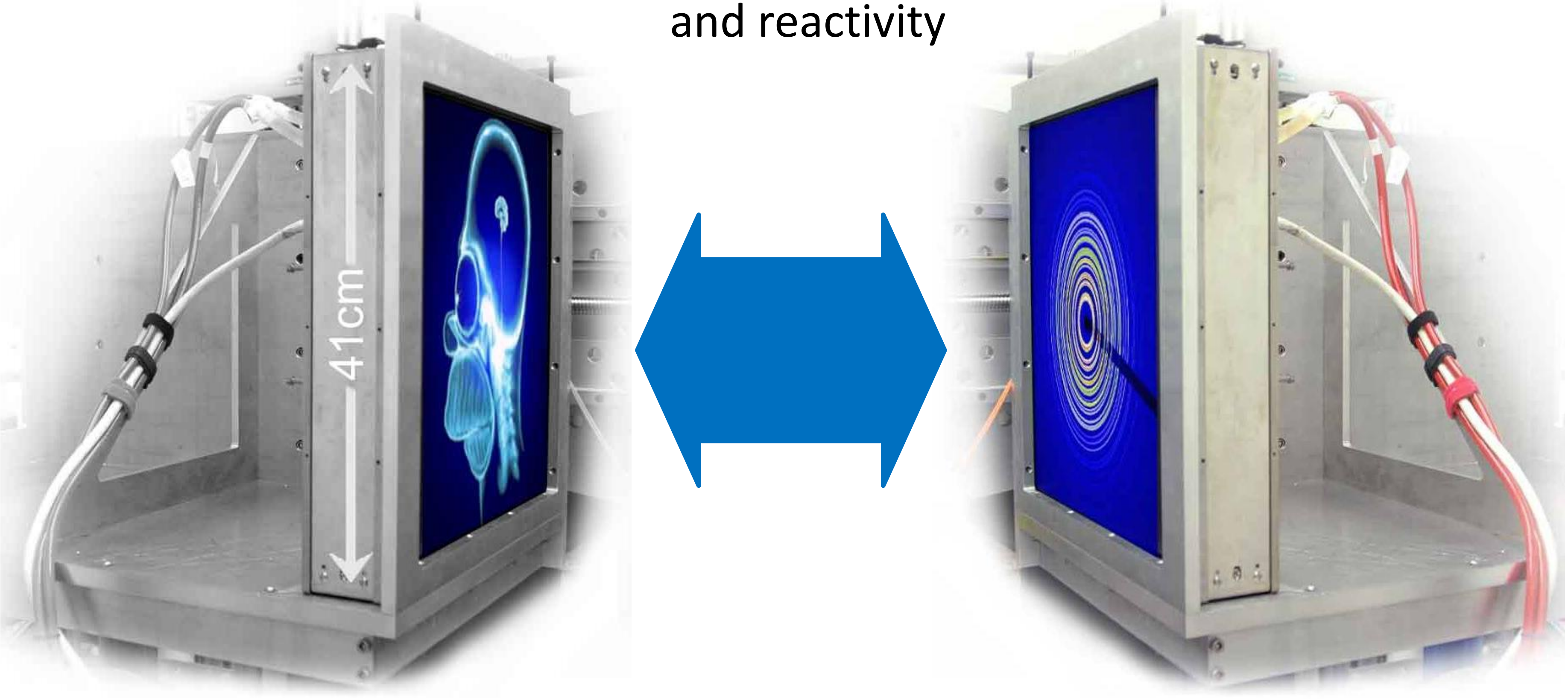

Exploring materials function with advanced tools

We probe the atomic structure of functional materials

During operation, reaction or changing environmental variable

To develop a predictive understanding of functional properties

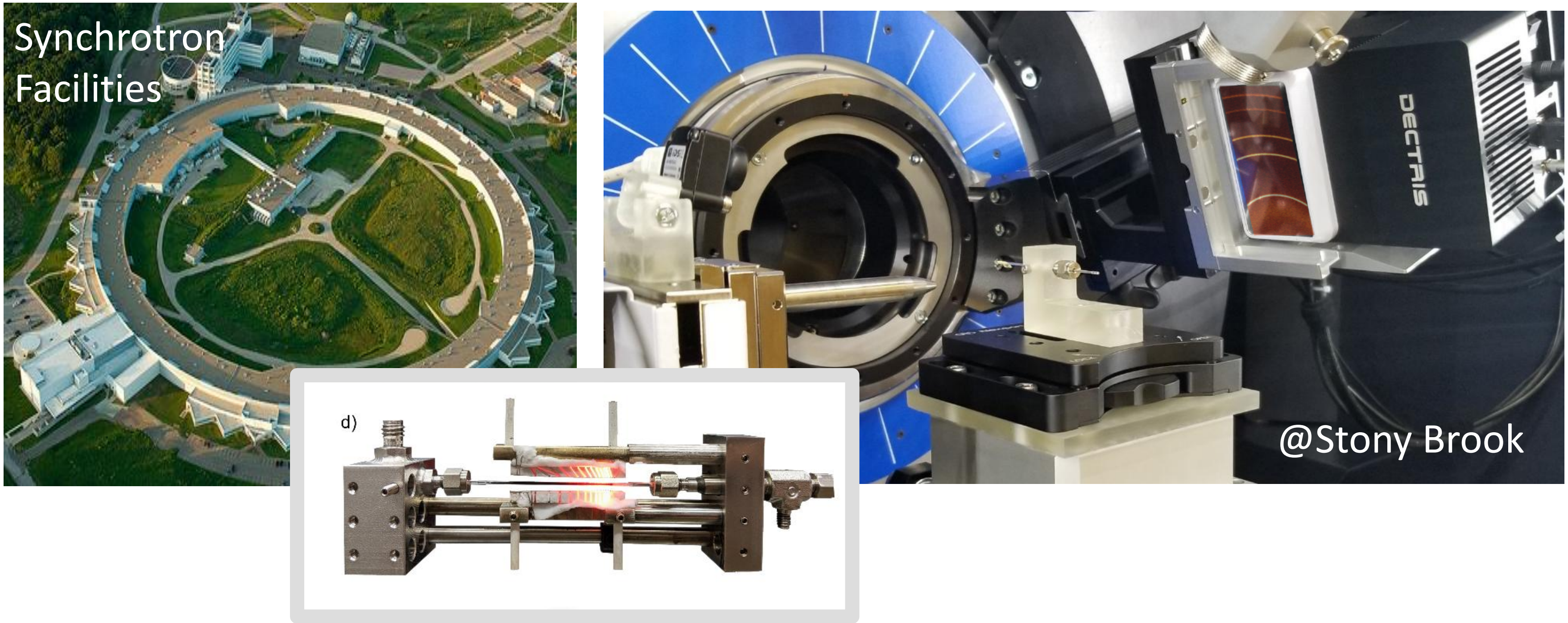

Multimodal correlation of local & long range structure

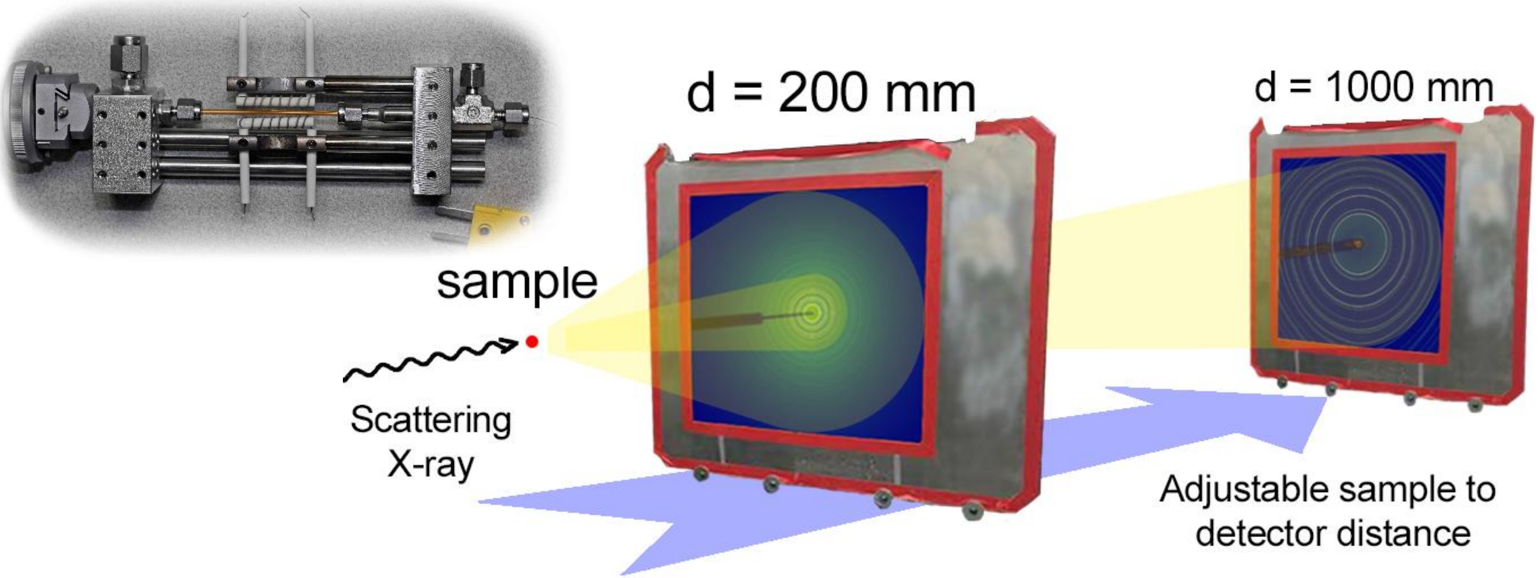

High-resolution
atom position for PDF

High-resolution
peak profile for XRD

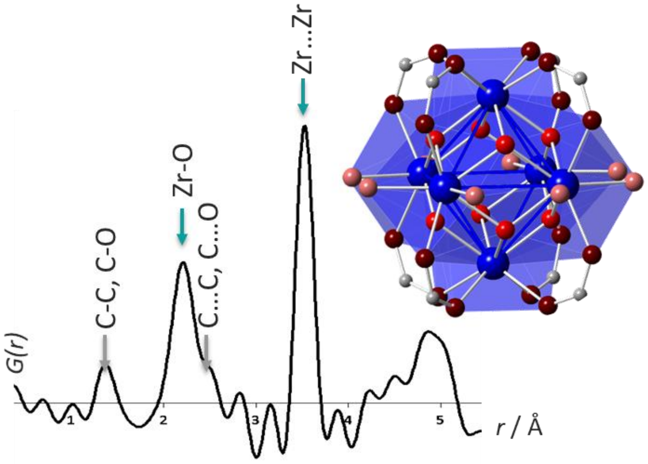

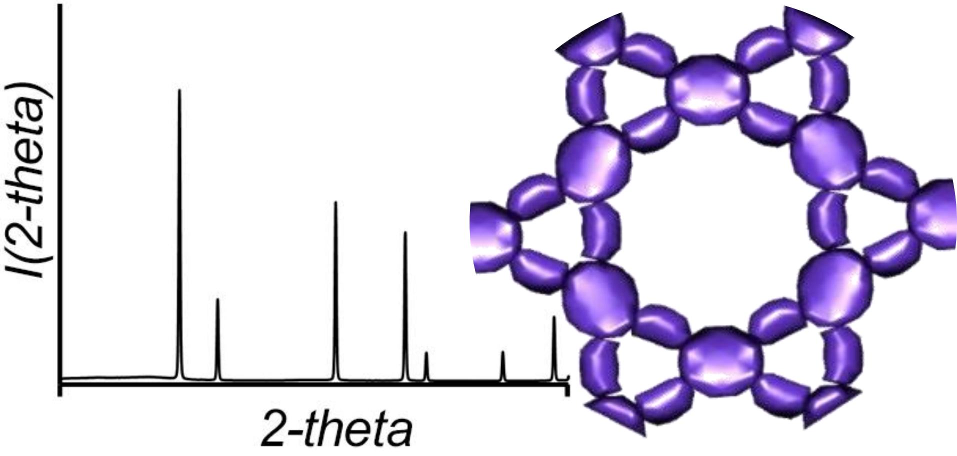

MOFs as a versatile platform for exploring catalysis

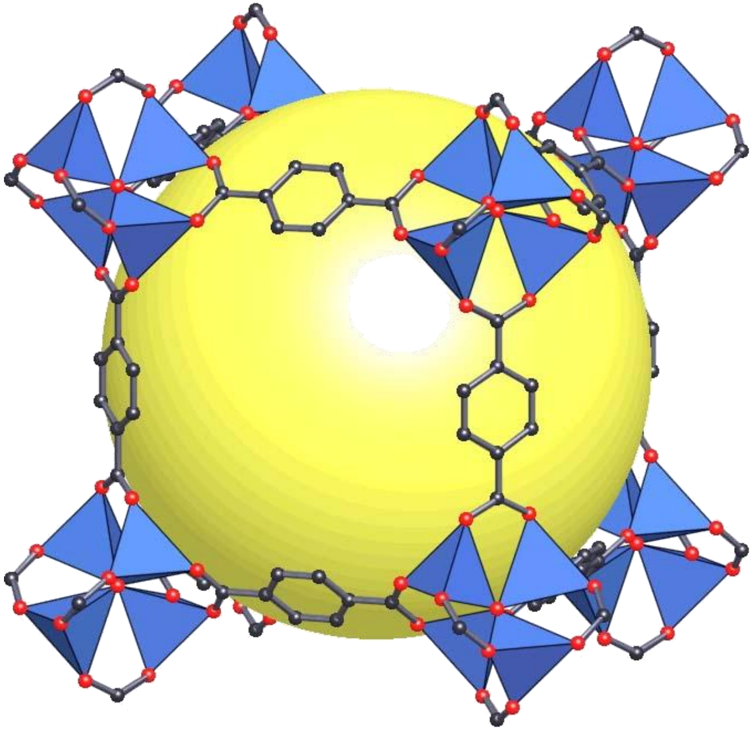

The crystallinity of the MOF lattice favors *chemically uniform* active sites.

This facilitates characterization and understanding of the catalyst structure-activity relationship

The MOF structure and chemistry can be tuned, and the surface functionalized to systematically explore catalysis

ICDC
INORGANOMETALLIC
CATALYST DESIGN CENTER

CATALYST DESIGN FOR DECARBONIZATION CENTER
H_2
CD4DC

NU-1000 MOF: A highly porous framework

A Northwestern University MOF

The metal-organic framework NU1000 is of interest as a catalyst and catalyst support

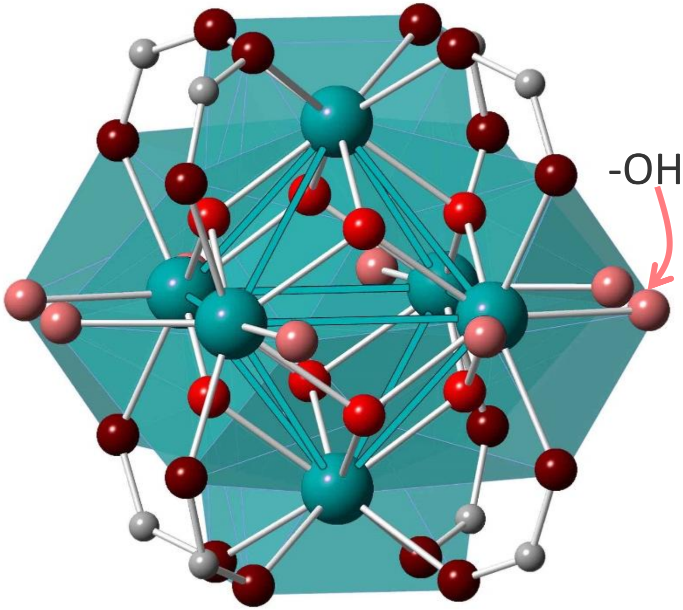

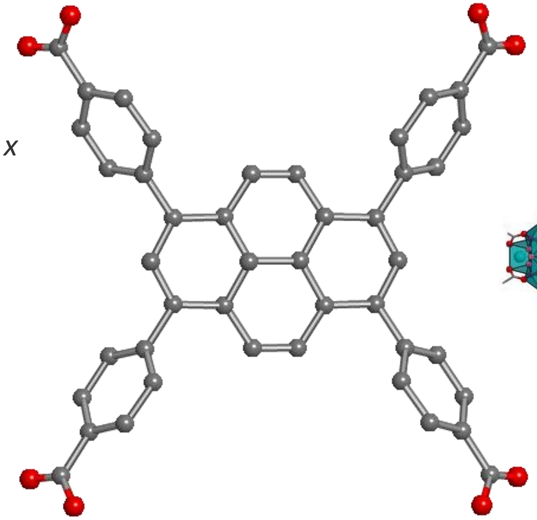

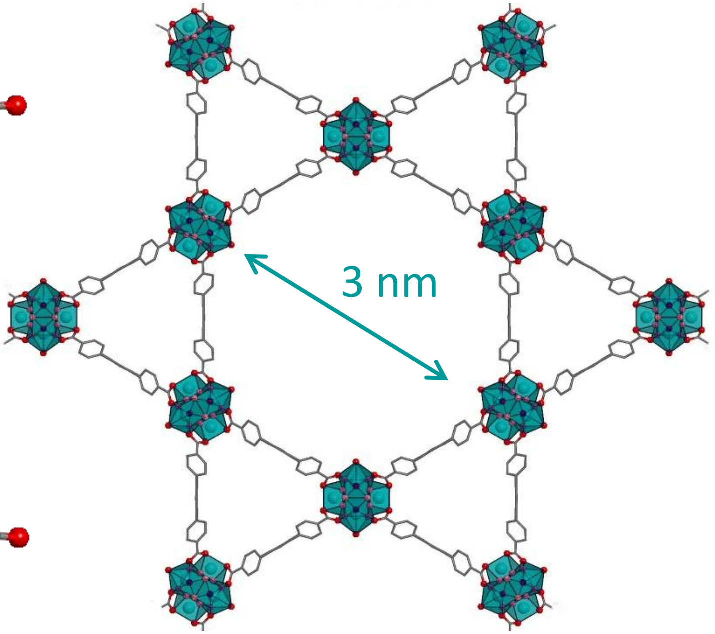

Zr_6O_8 node + **Pyrene-based ligand** = **NU-1000 MOF**

Farha, Hupp *et al. J. Am. Chem. Soc.*, **2013**, *135*, 10294–10297

J. Am. Chem. Soc., **2016** 4178–4185

Subtle changes to powder diffraction

The strength of Zr^{IV}-O bonds within zirconia nodes imparts high stability to NU-1000, allowing it to tolerate reaction conditions.

There are no obvious changes to crystal symmetry/structure.

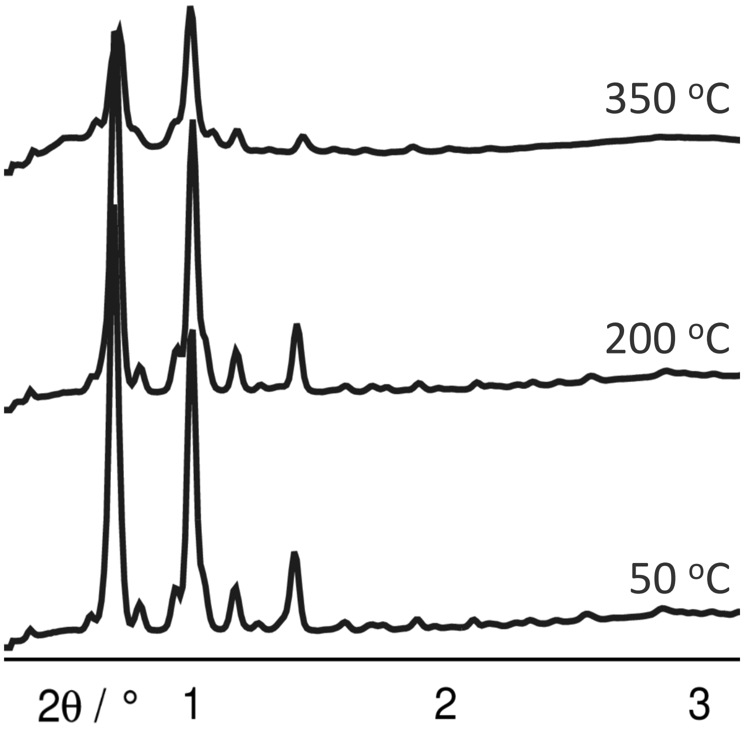

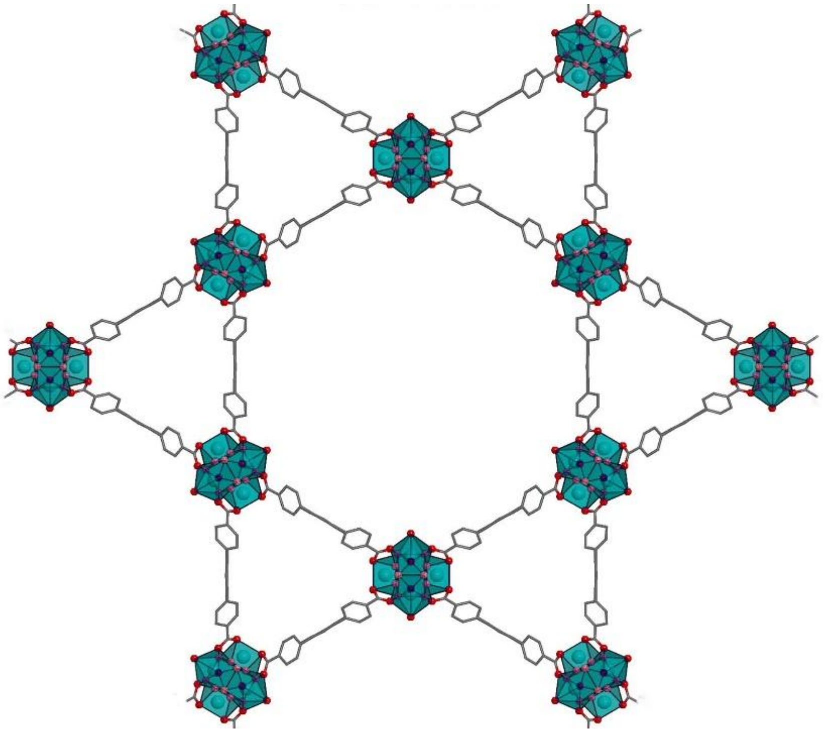

J. Am. Chem. Soc., **2016** 4178–4185

A local structure picture from PDF

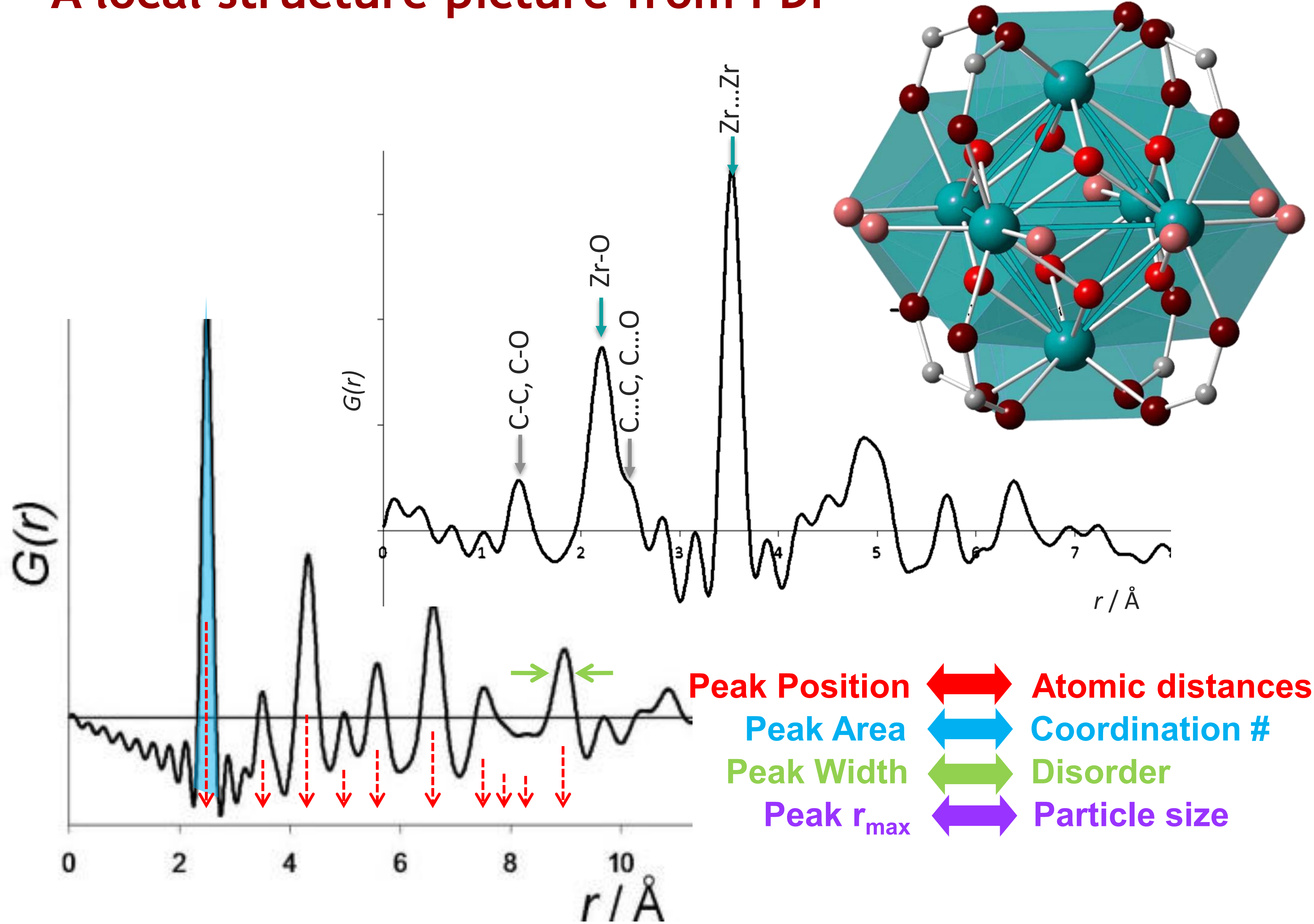

Peak Position ⟷ Atomic distances

Peak Area ⟷ Coordination #

Peak Width ⟷ Disorder

Peak r_{max} ⟷ Particle size

J. Am. Chem. Soc., **2016** 4178–4185

PDF identifies a large irreversible transition

Variable temperature PDF studies reveal
an unexpected and irreversible change in the local atomic structure
– reducing the symmetry of the Zr_6-based nodes.

Zr_6O_8 nodes, while chemically robust are not static

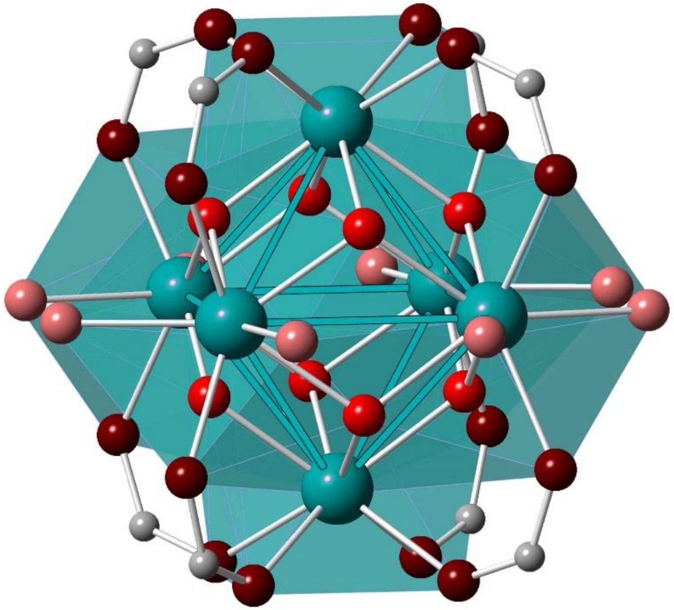

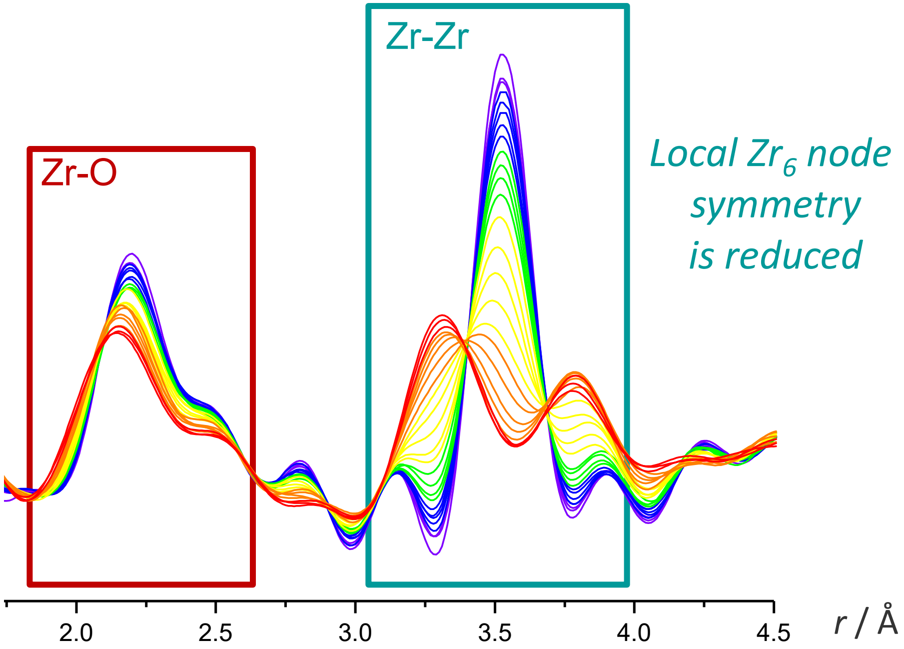

Experimental PDF data collected at 11-ID-B
at the Department of Energy's Advanced Photon Source
heating from 50 ˚C to 350 ˚C

Consider the phase transitions of zirconia

Transitions between cubic, tetragonal and monoclinic forms of bulk zirconia occur at high temperature

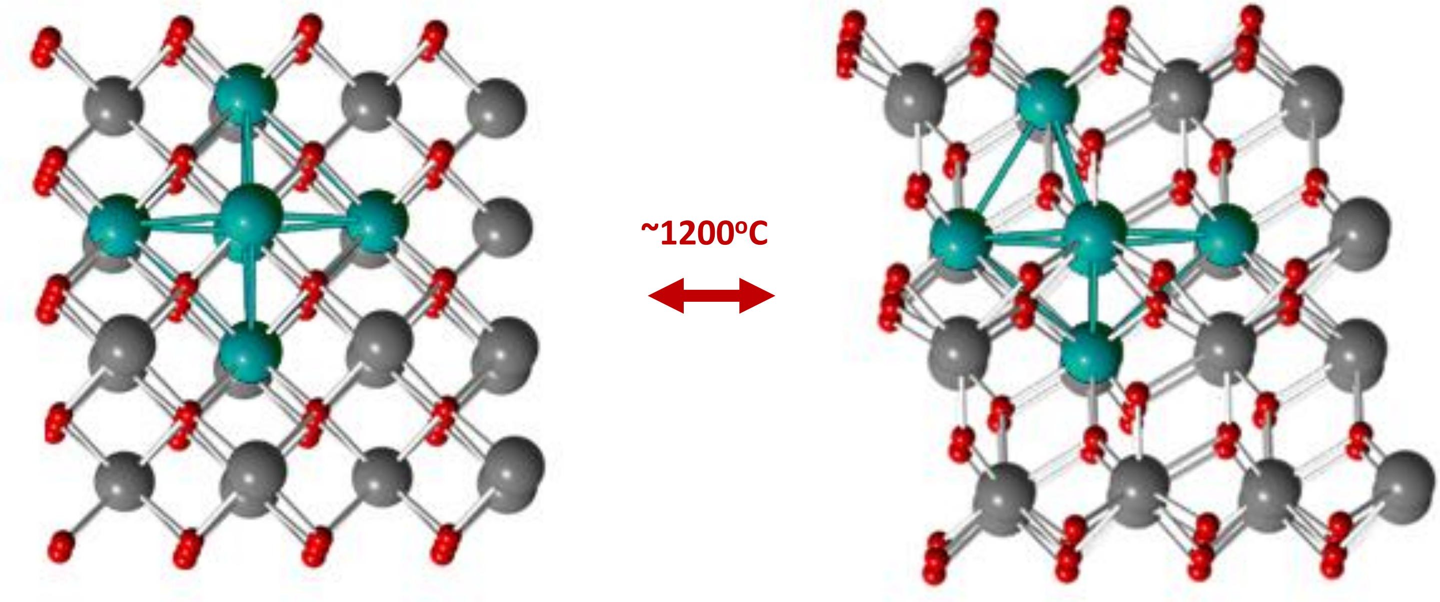

J. Am. Chem. Soc., **2016** 4178–4185

MOF nodes are the ultimate nanoparticles

Local structure changes within node
matches those in **bulk zirconia,**
but occur at much **lower temperatures**
and in the **reverse direction**.

Distorted node is more catalytically active

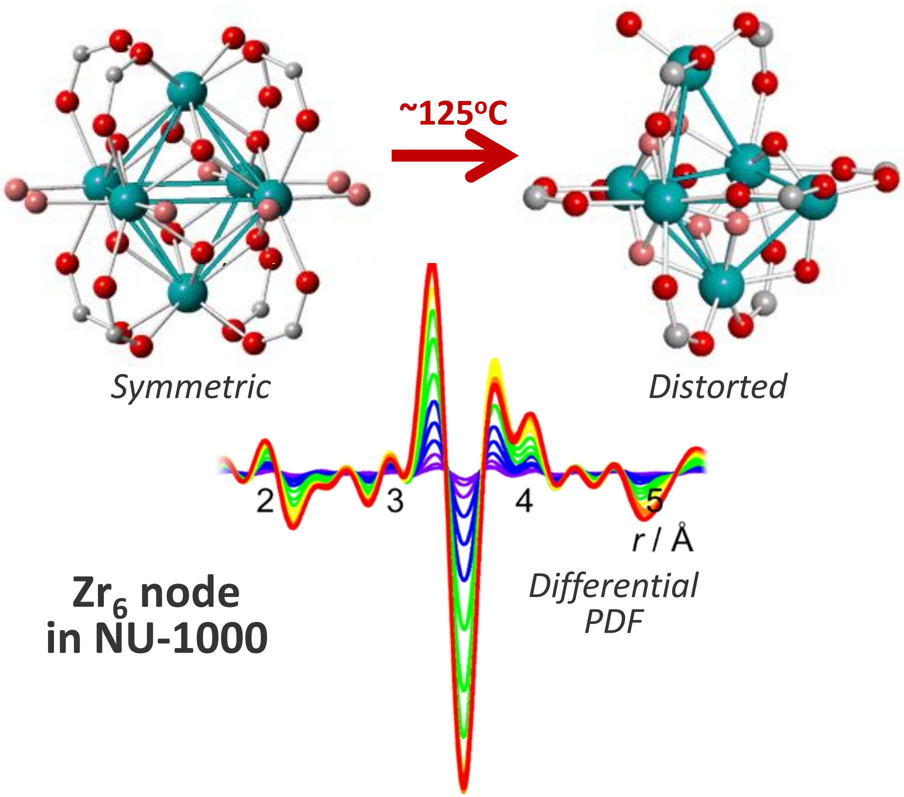

Zr_6 node in NU-1000

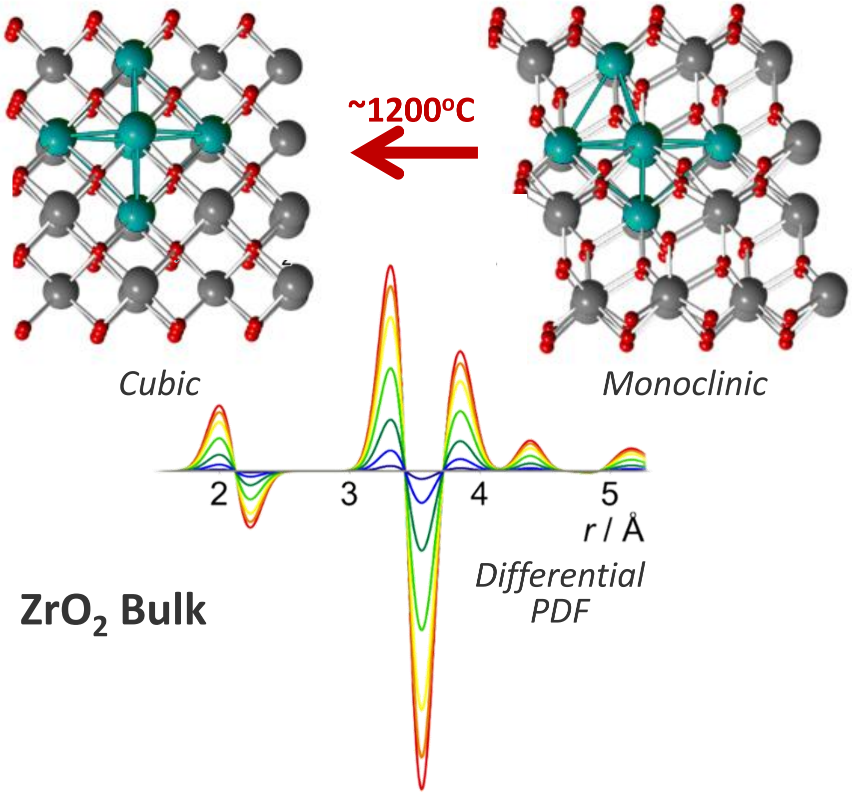

ZrO_2 Bulk

Chemical functionalization of the node

Joe Hupp

NORTHWESTERN UNIVERSITY
QUAECUMQUE SUNT VERA
1851

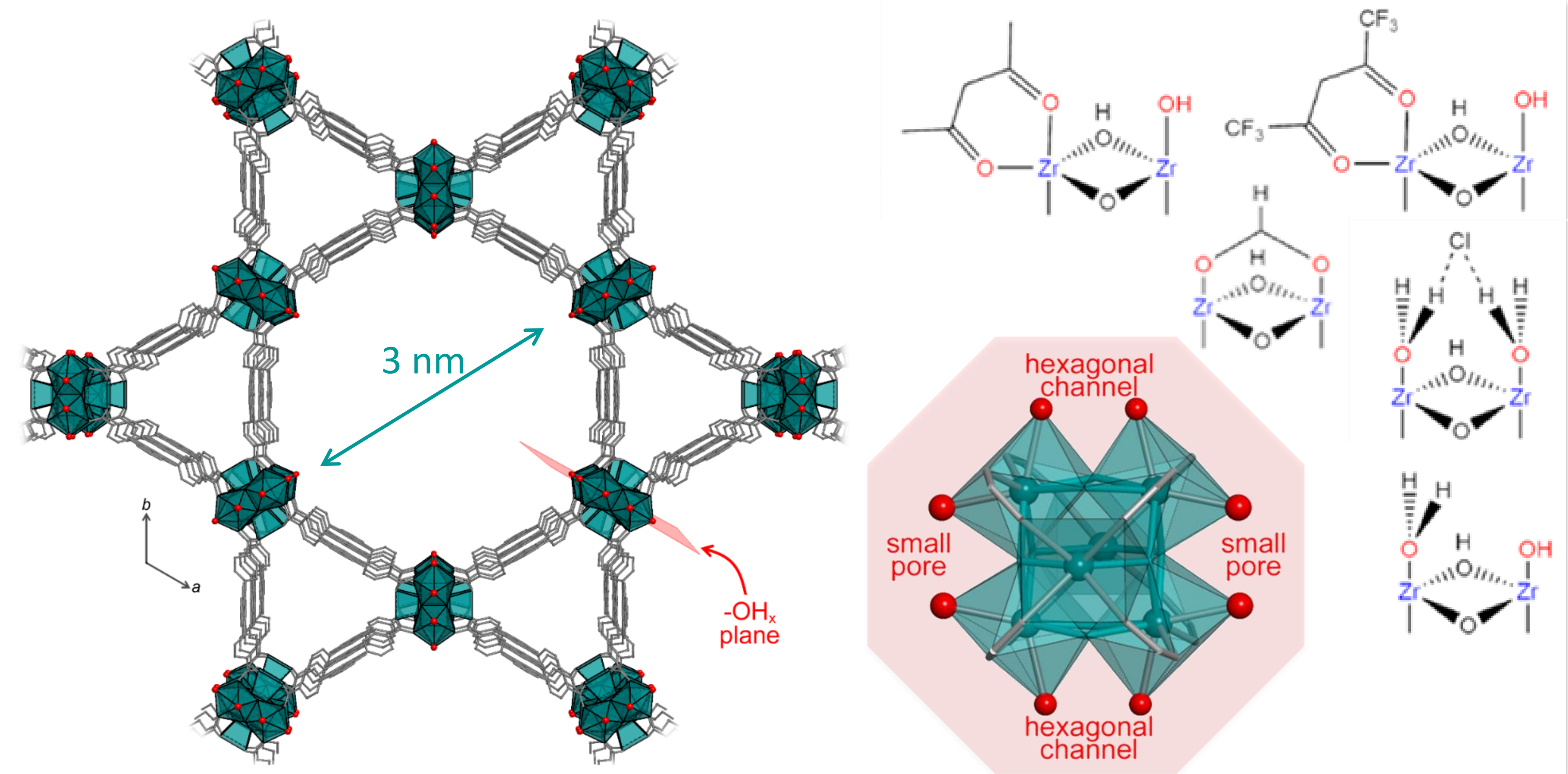

Decorated NU-1000s have same structure

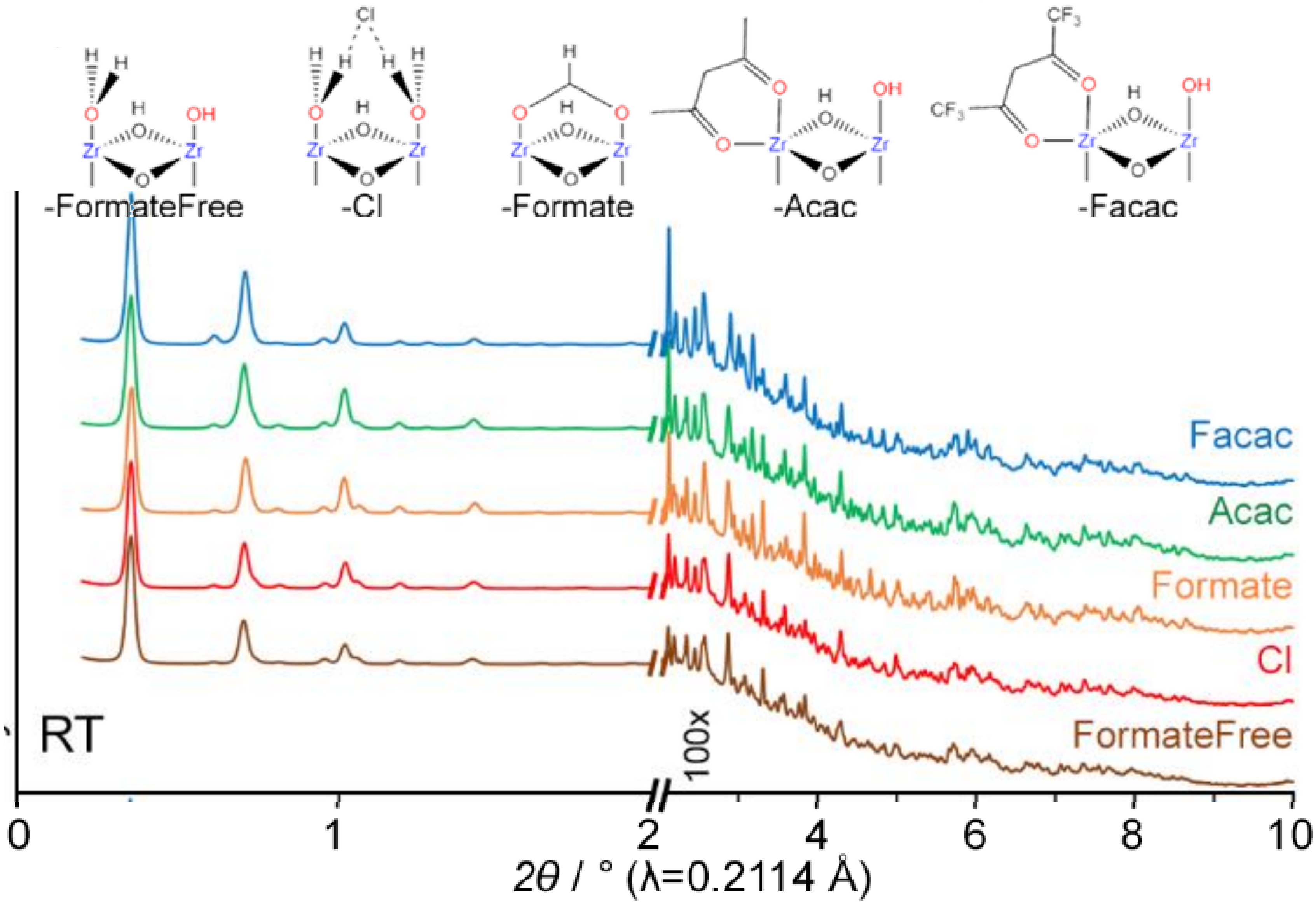

Decorated NU-1000s have same structure

But different temperature dependence

-Cl and Formate free NU-1000 lose crystallinity at 250 ^oC

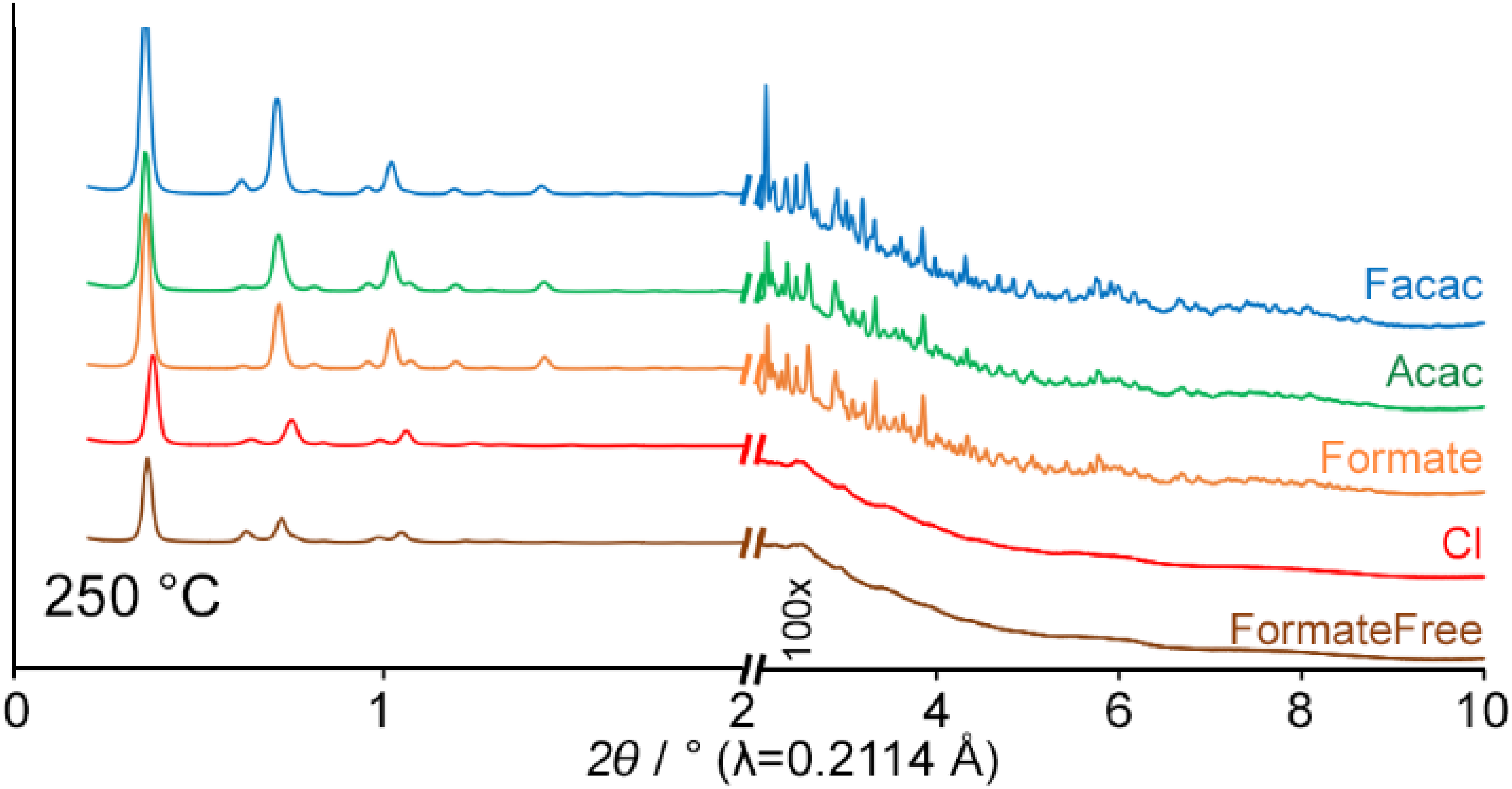

J. Am. Chem. Soc. 2023, 145, 1, 268–276

Zr_6 node distorts reversibly

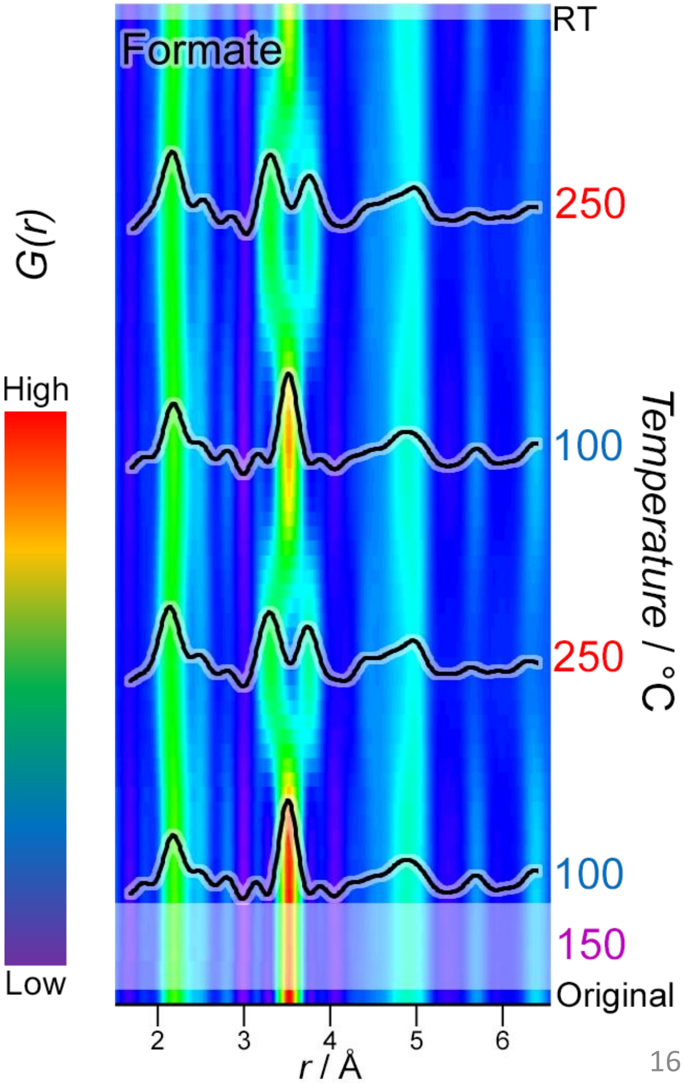

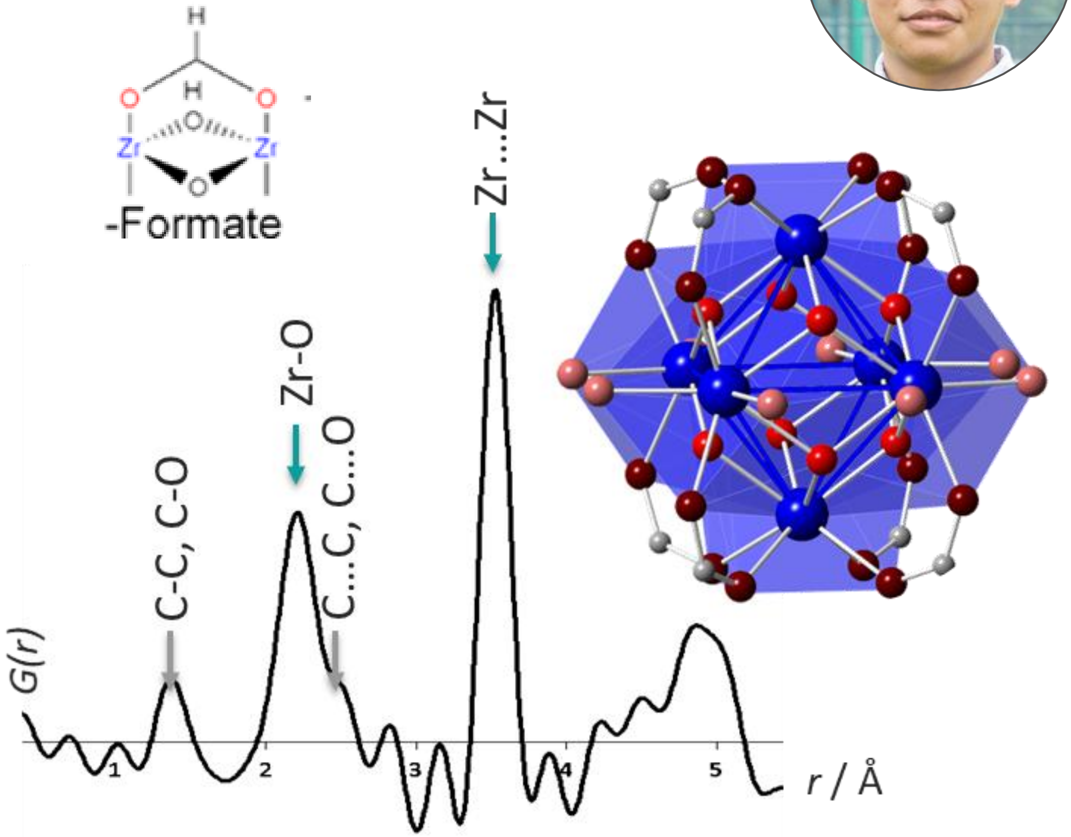

PDF - Local structure independent of crystallinity

Peak Position ↔ **Atomic distances**
Peak Area ↔ **Coordination #**
Peak Width ↔ **Disorder**

J. Am. Chem. Soc. 2023, 145, 1, 268–276

PDF shows different node distortions

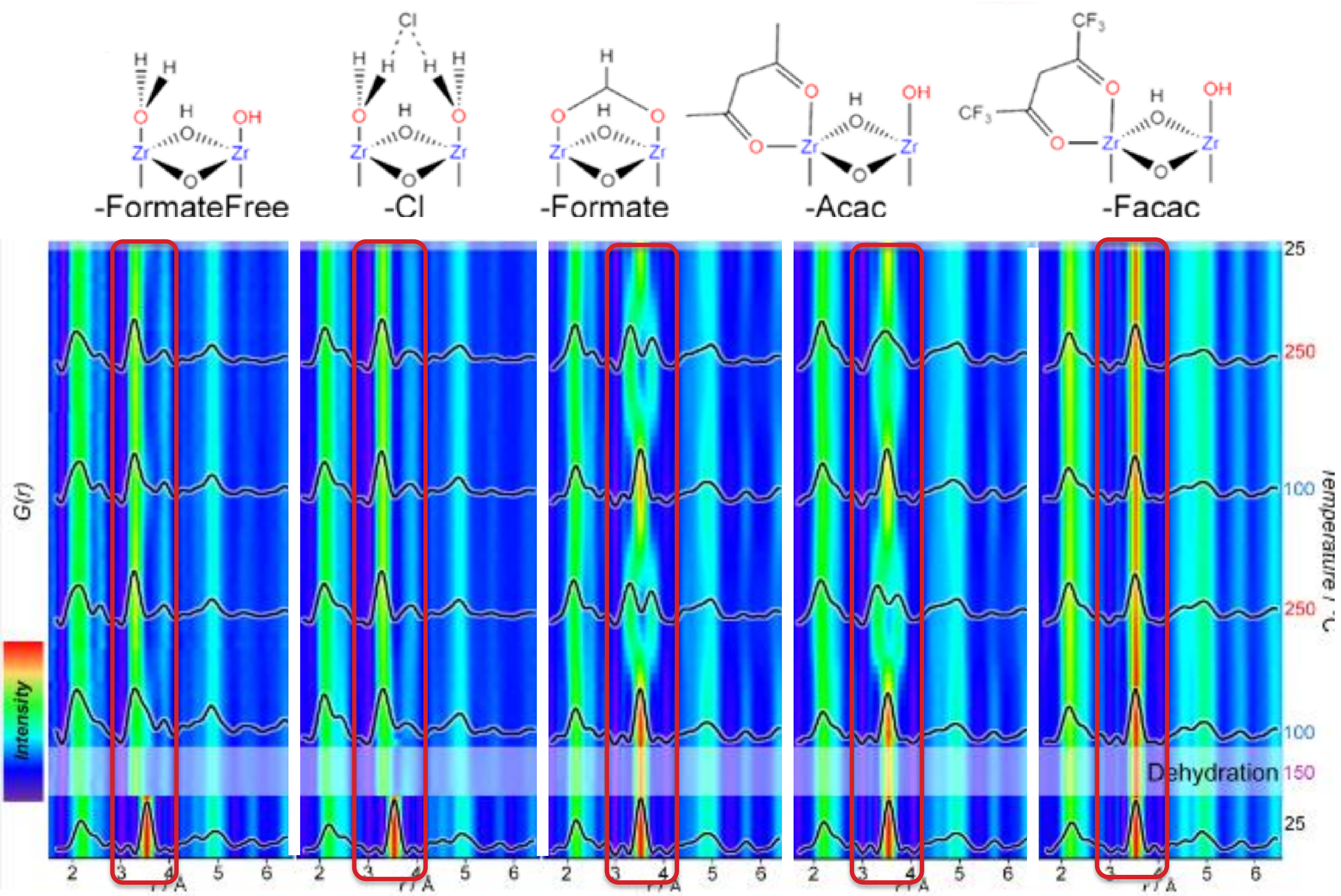

Multivariate analysis separates distinct local states

Dimensional reduction algorithms such as Non-Negative Matrix Factorization (NMF) cluster features that change together

This provides a model-free approach to separate and quantify distinct “states” or phases of the system.

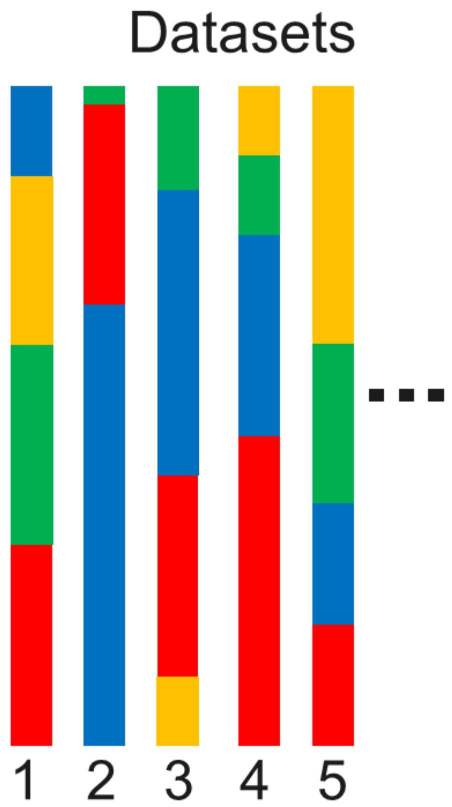

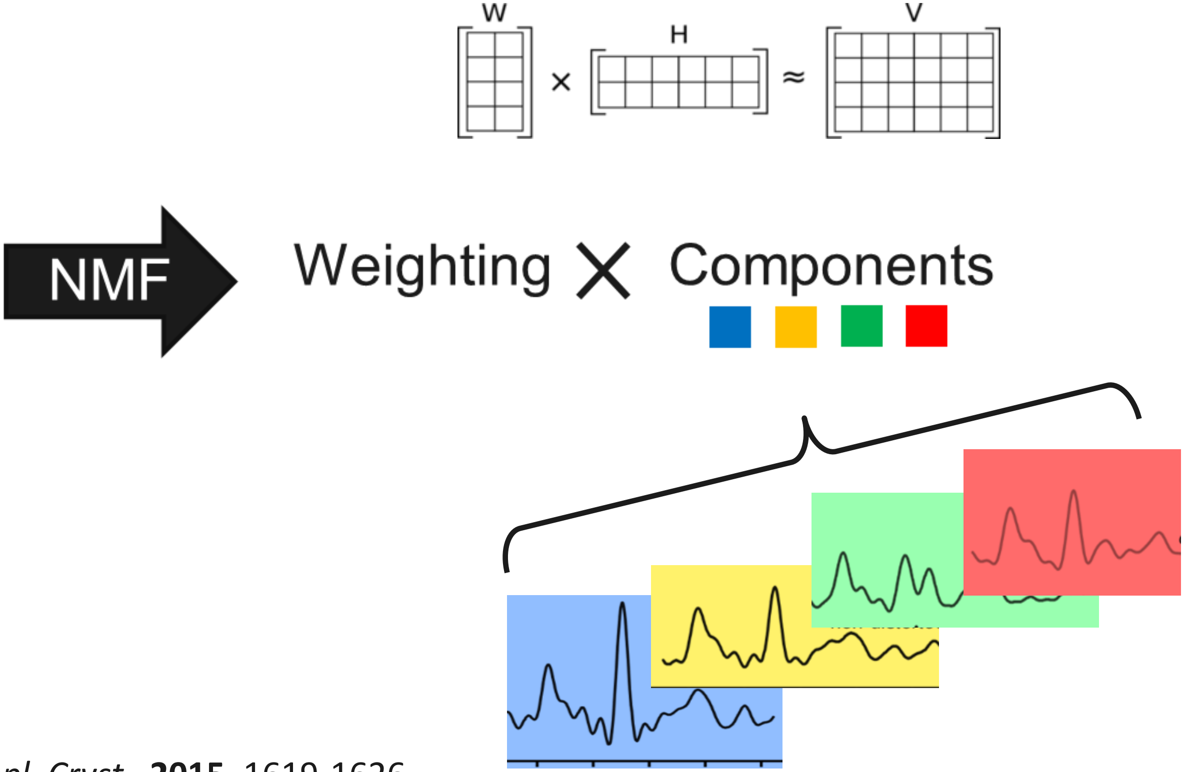

J. Appl. Cryst, **2015**, 1619-1626
J. Appl. Cryst. **2020** 662-670

J. Am. Chem. Soc. 2023, 145, 1, 268–276

Multivariate analysis decouples distinct states

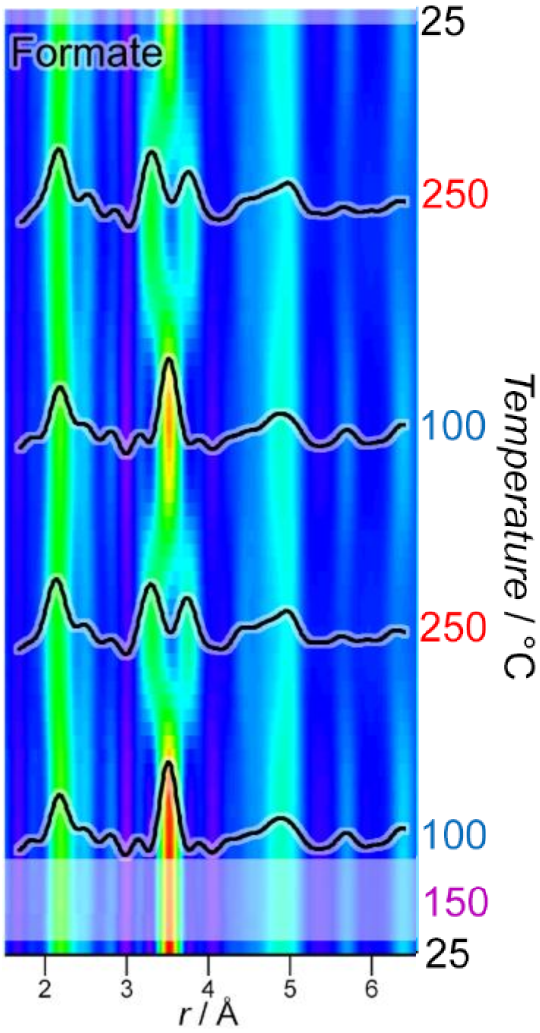

Simplifies data by isolating the components of the data that change together,

and re-factorizes the data as those discrete components and their time-dependent weightings

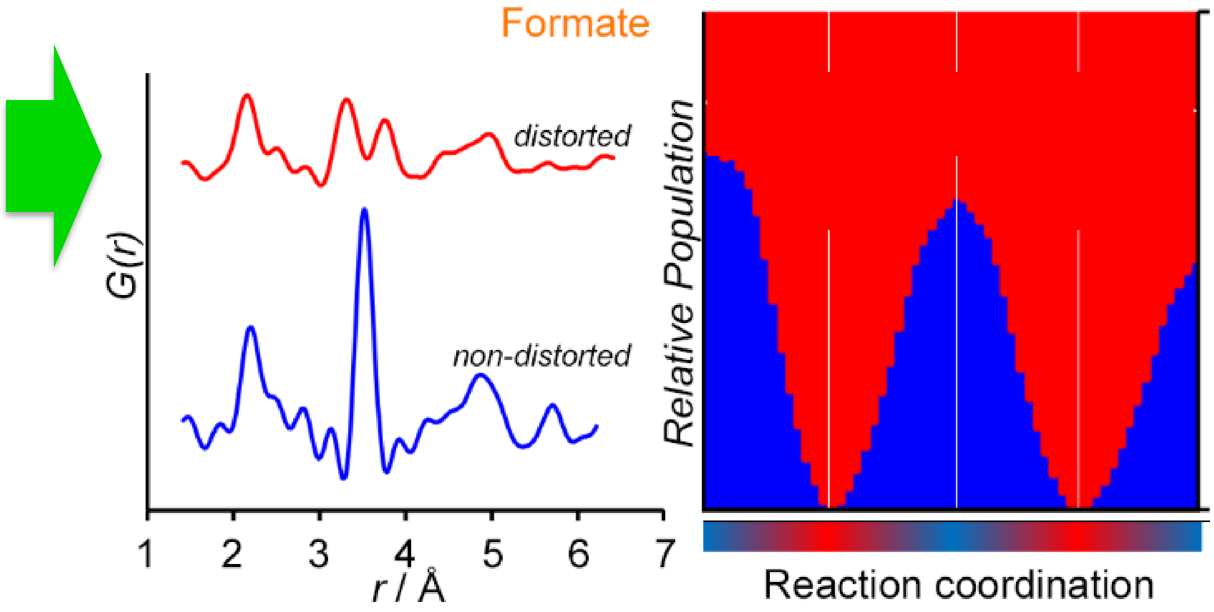

J. Am. Chem. Soc. 2023, 145, 1, 268–276

Local distortion linked to long-range lattice flexing

Thermal expansion
along the a axis is
directly correlated with
the distorted node population

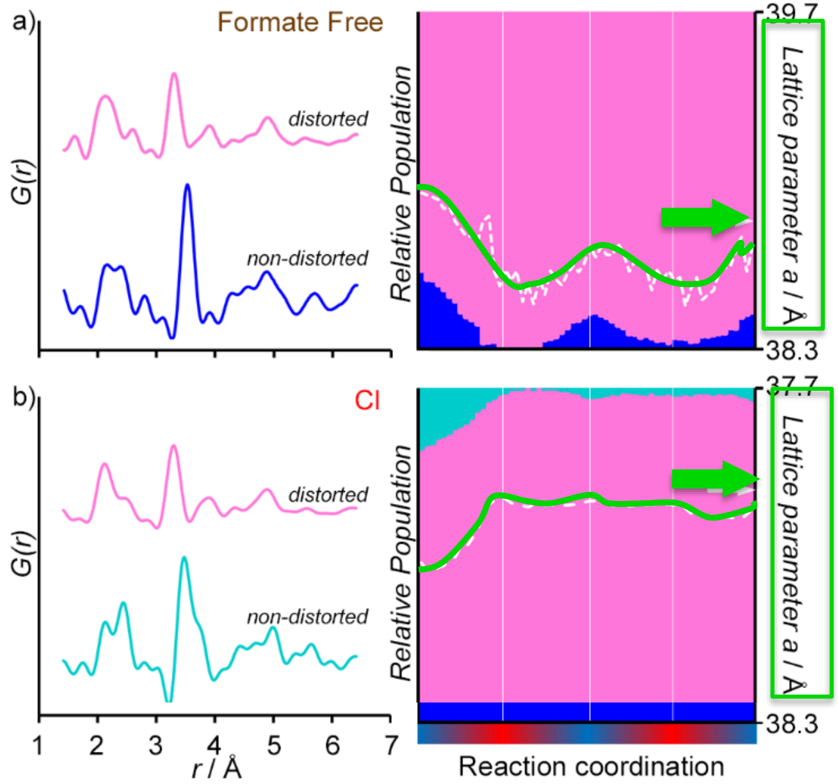

Contract with heating

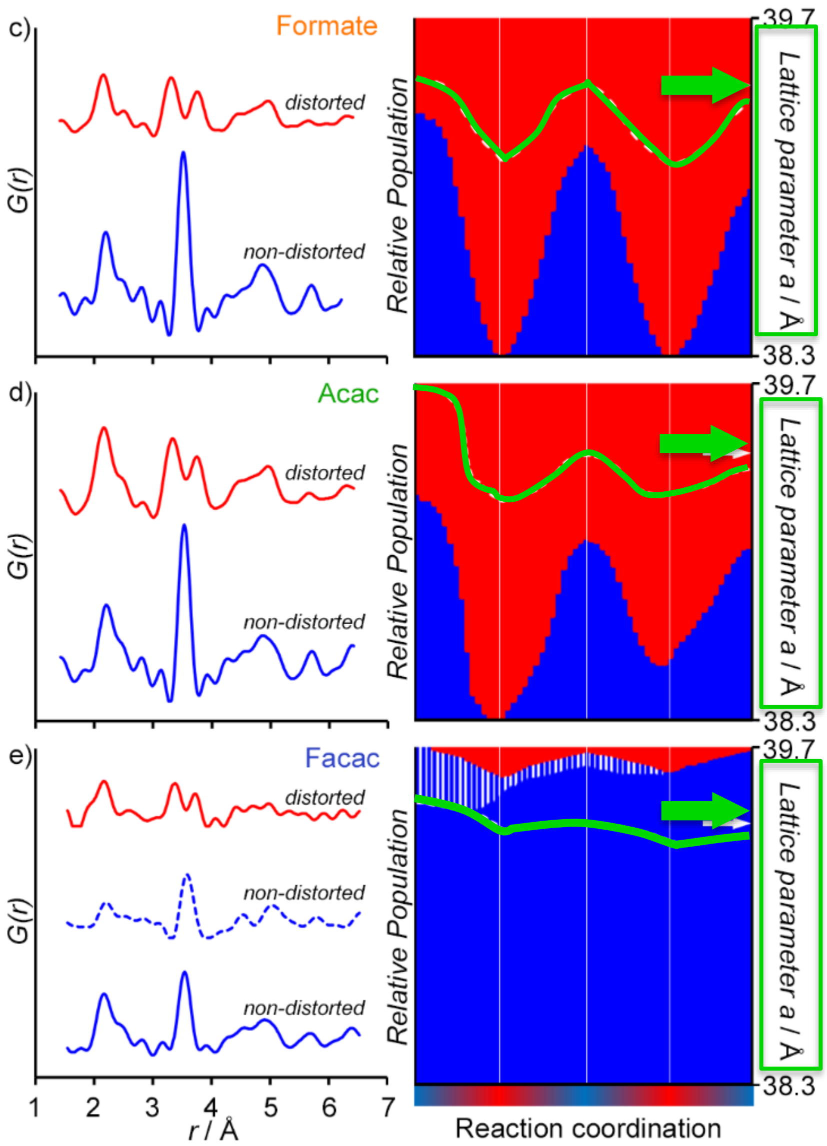

Thermal Expansion - What is normal?

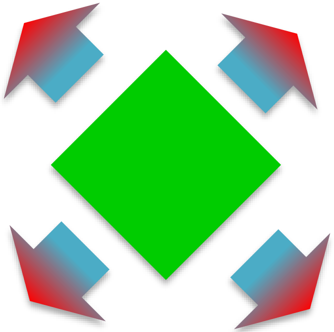

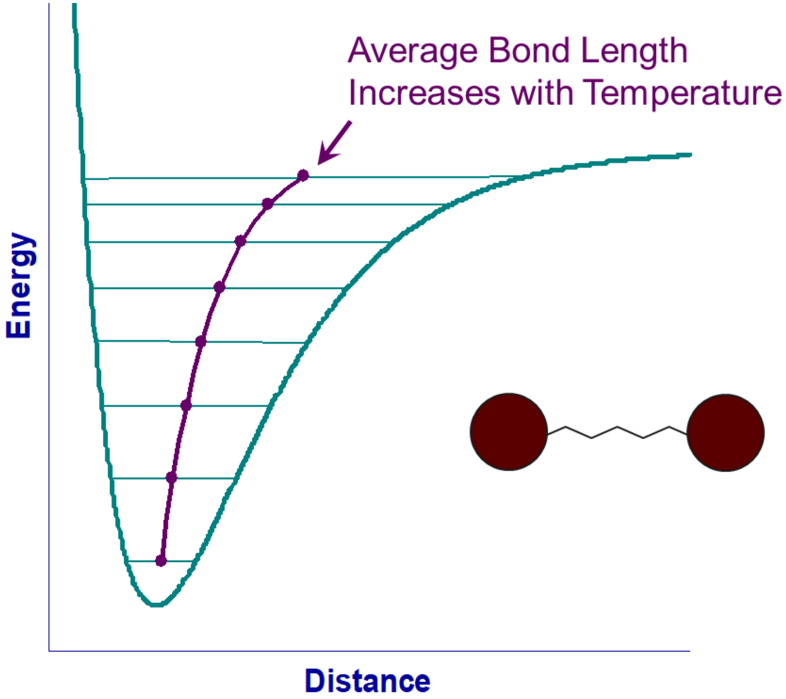
Average Bond Length Increases with Temperature

J. Am. Chem. Soc. 2023, 145, 1, 268–276

Node distortion as a novel mechanism for NTE

<u>Negative thermal expansion</u> along the a axis is directly correlated with the distorted node population

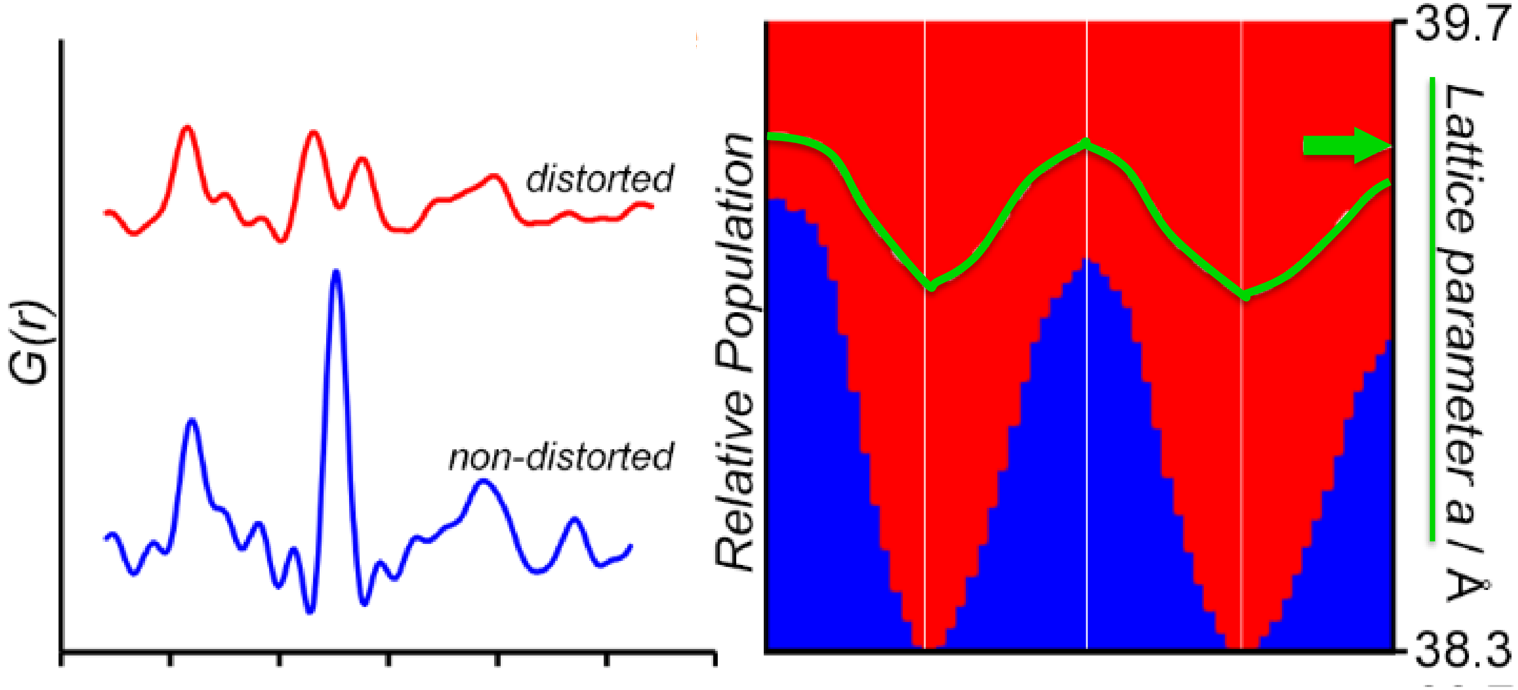

Contract with heating
Expand with cooling

J. Am. Chem. Soc. 2023, 145, 1, 268–276

Node distortion as a novel mechanism for NTE

Increasing the relative population of distorted (smaller) nodes with increasing temperature leads to a contraction of the MOF lattice

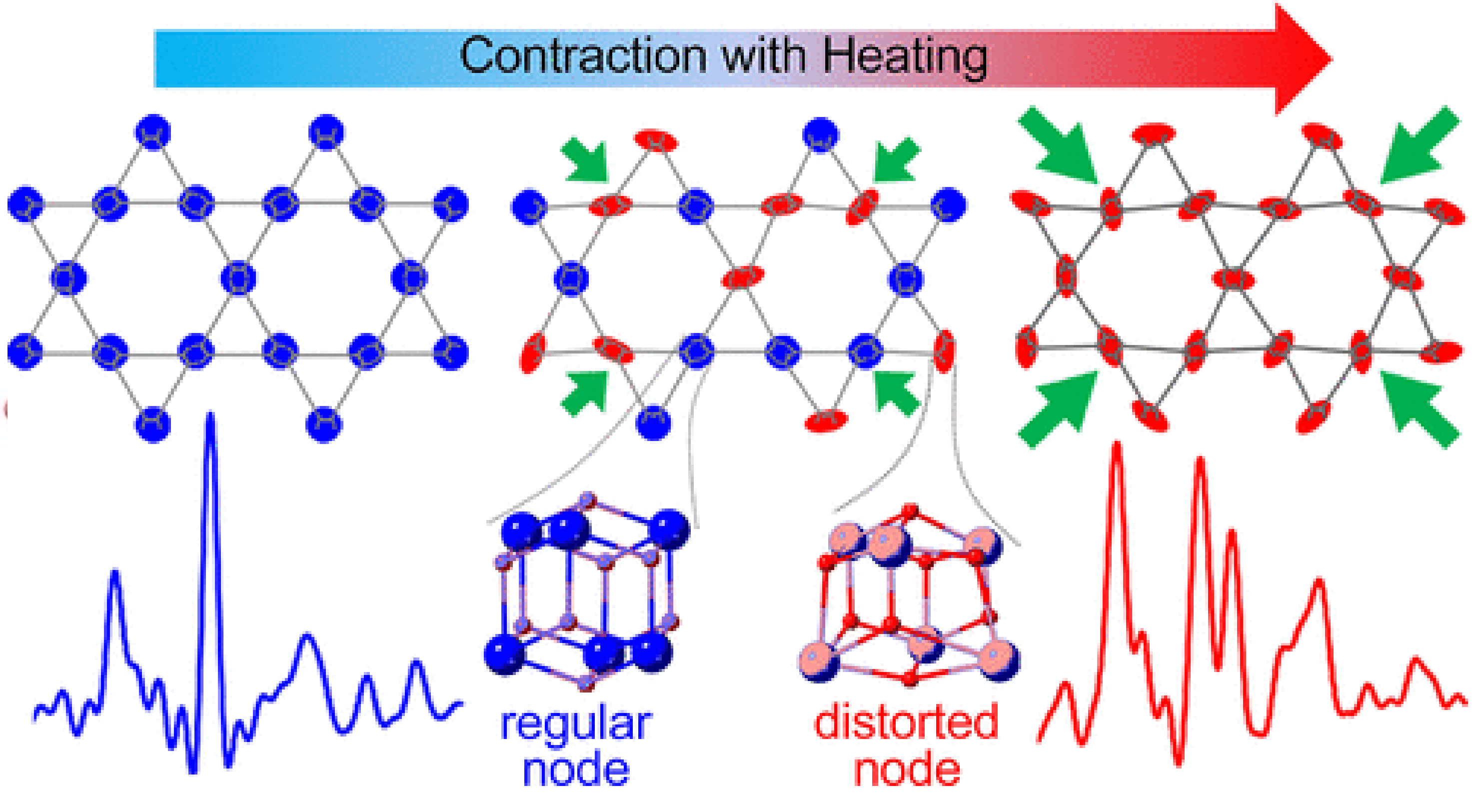

larger

smaller

J. Am. Chem. Soc. 2023, 145, 1, 268–276

Node distortion as a novel mechanism for NTE

Increasing the relative population of distorted (smaller) nodes with increasing temperature leads to a contraction of the MOF lattice.

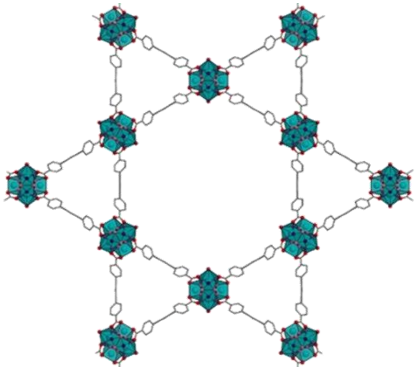

Distinct from established NTE mechanisms

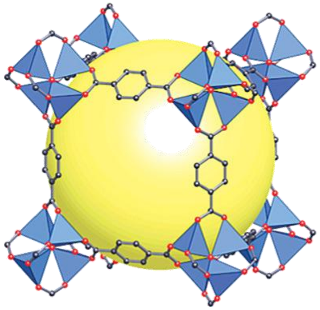

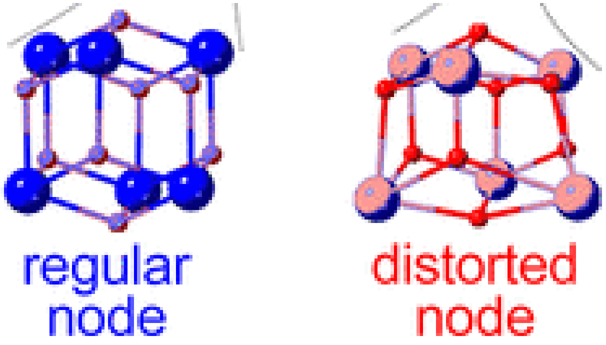

larger

smaller

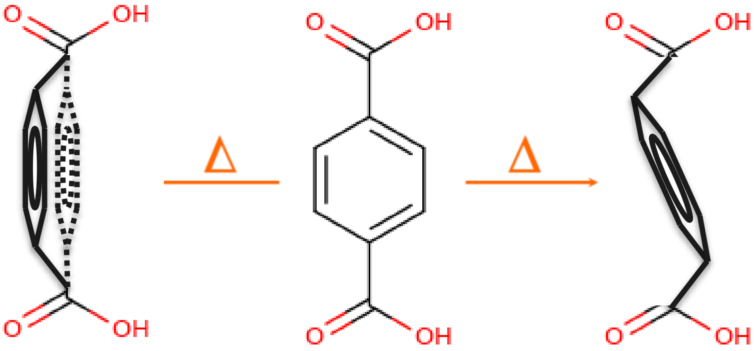

Zr_6 nodes in other MOFs

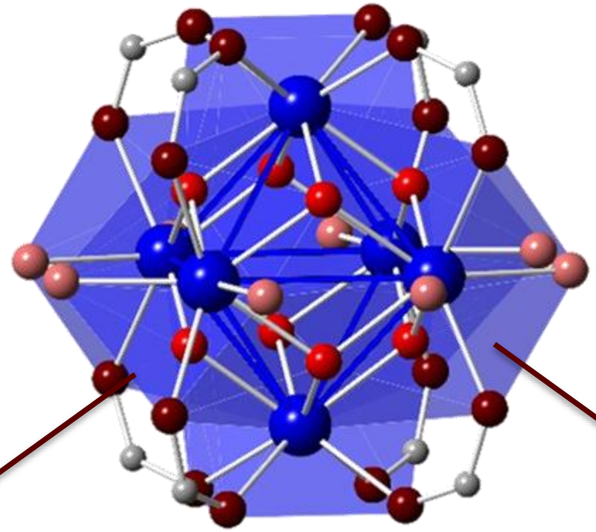

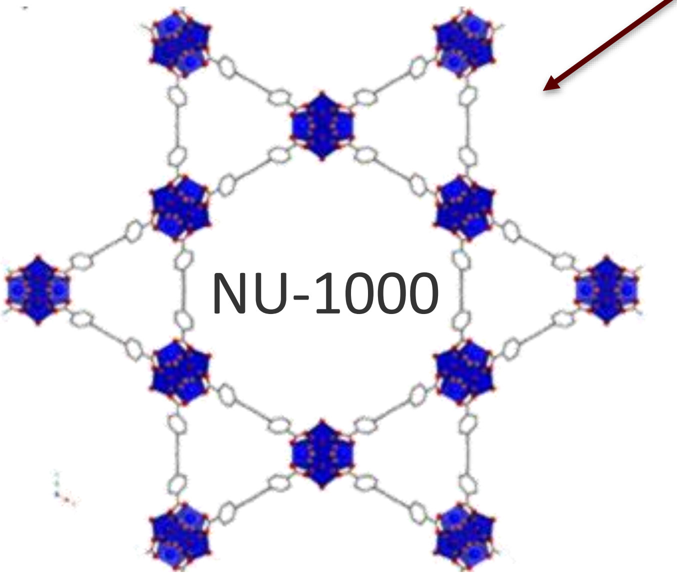

NU-1000

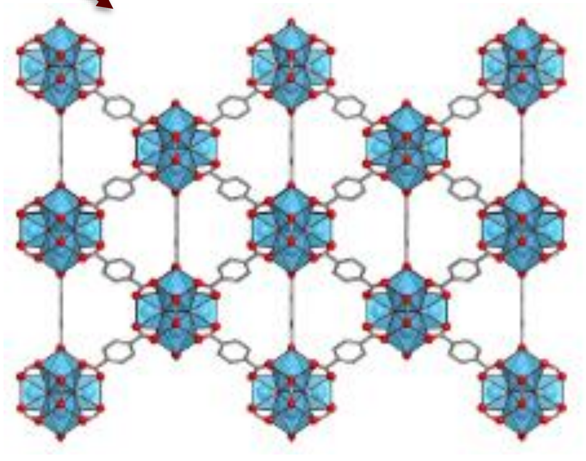

UiO-66

J. Am. Chem. Soc. **2024**, 16977

Evaluating NTE in UiO66

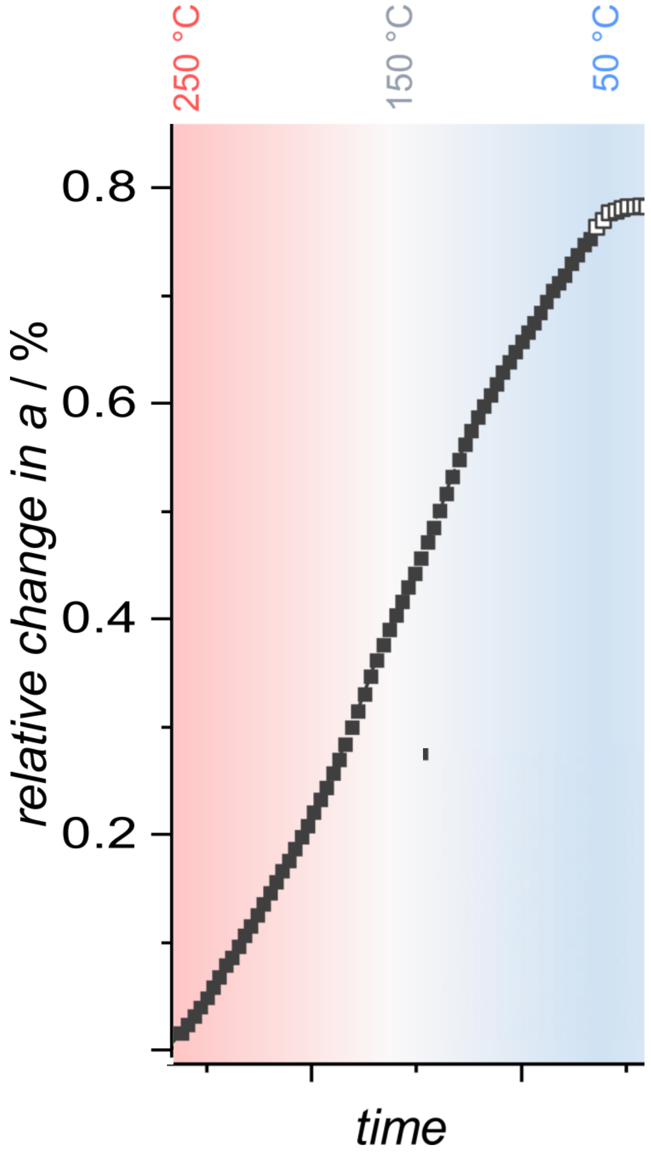

UiO-66 shows isotropic NTE.

The lattice expands as the temperature decreases

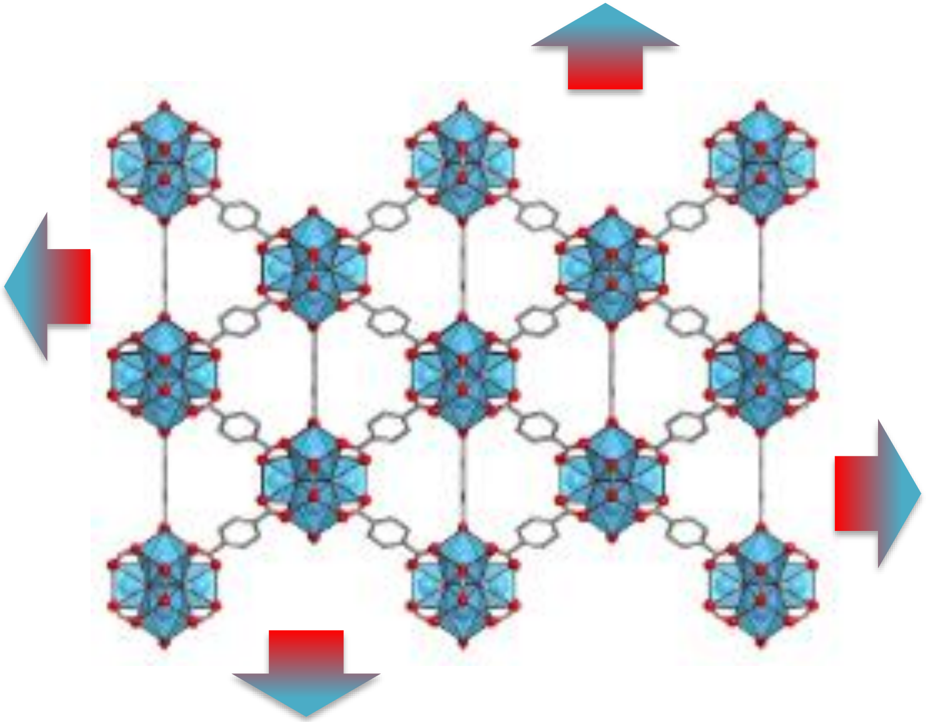

J. Am. Chem. Soc. **2024**, 16977

Evaluating NTE in UiO66, the original Zr_6-MOF

Simon Vornholt

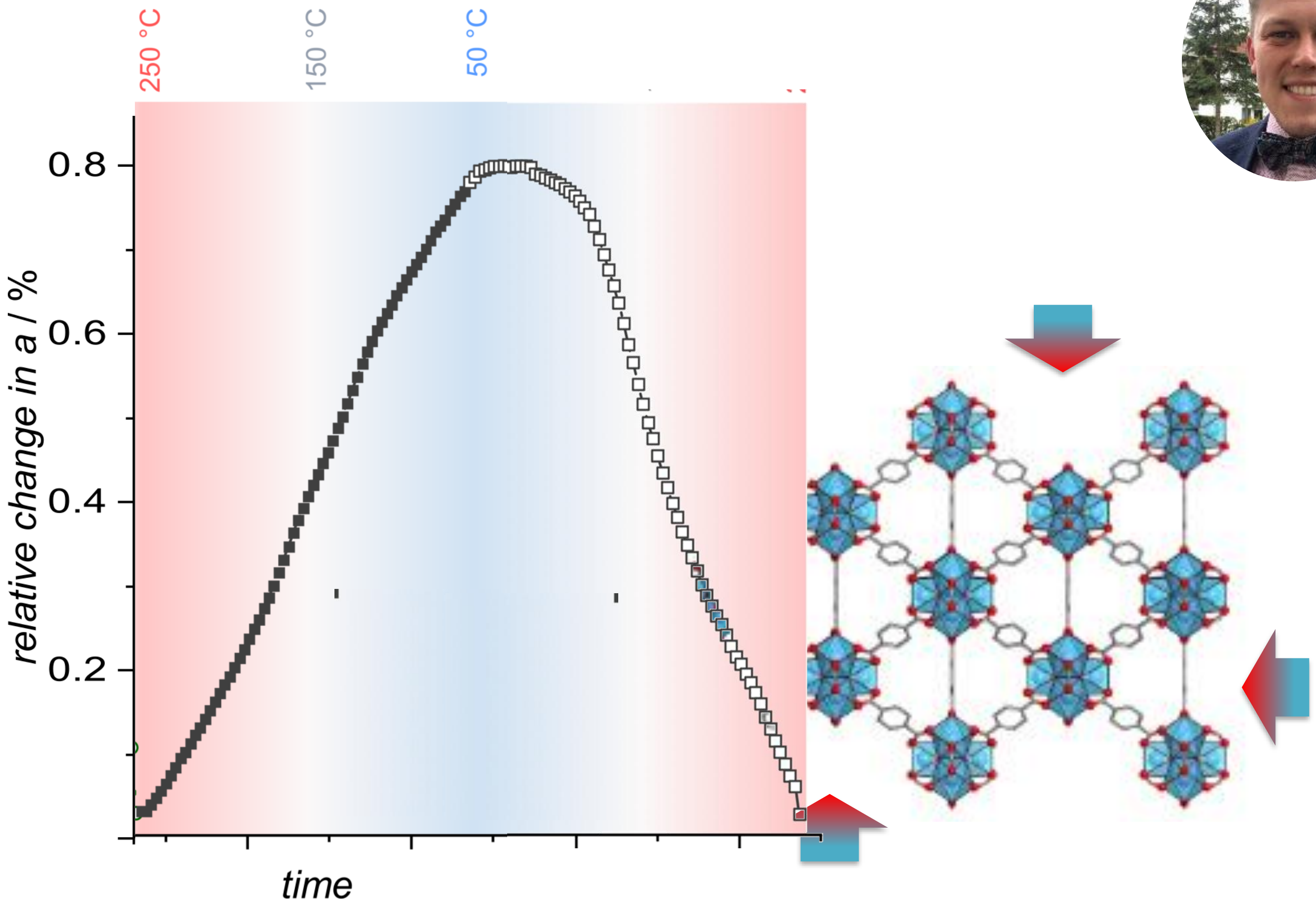

J. Am. Chem. Soc. **2024**, 16977

Unexpected hysteresis

Pronounced hysteresis in the cubic UiO-66 lattice dimension is evident between cooling and heating steps

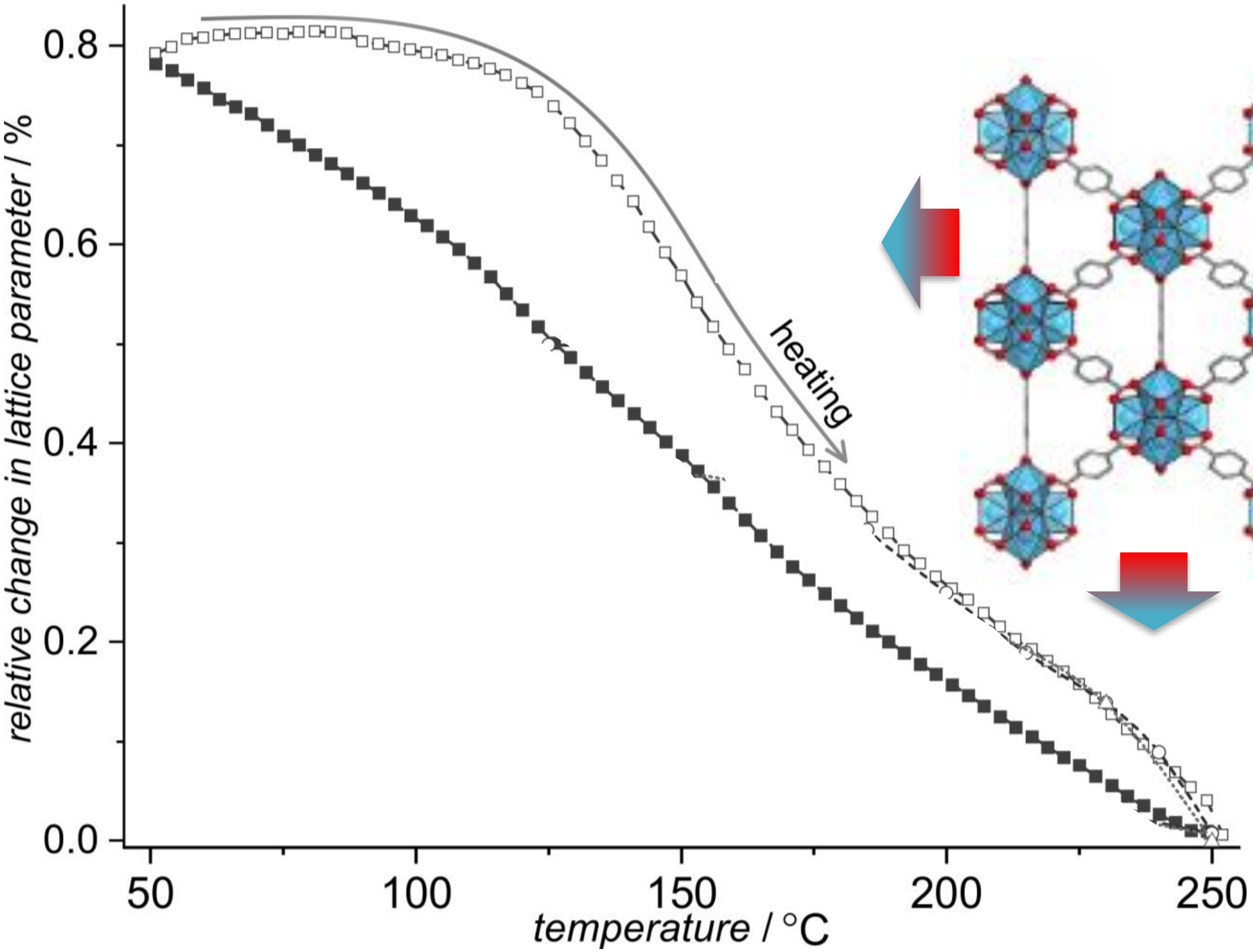

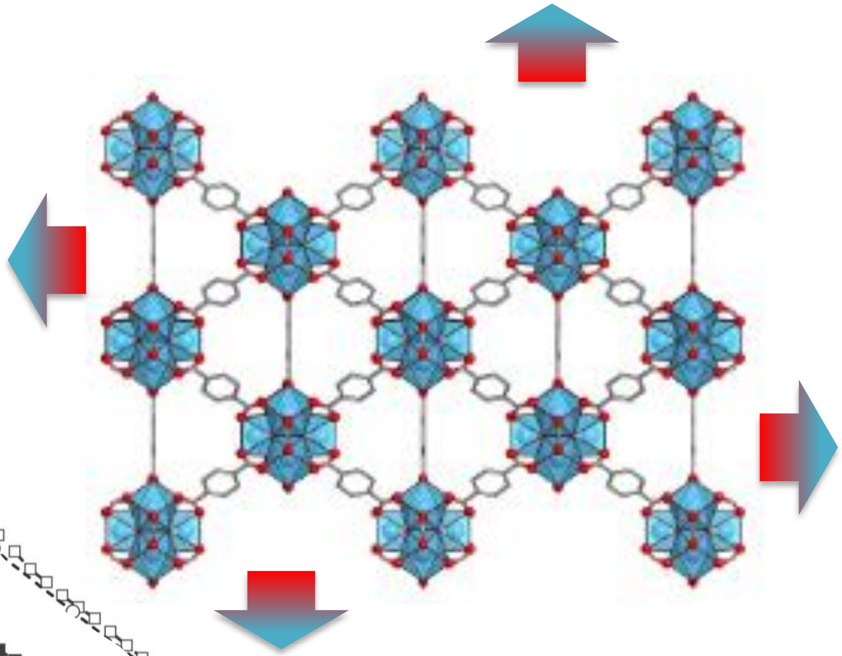

J. Am. Chem. Soc. **2024**, 16977

Unexpected hysteresis & rate-dependence

The hysteresis and apparent thermal expansion depend on both the thermal history and ramp rates

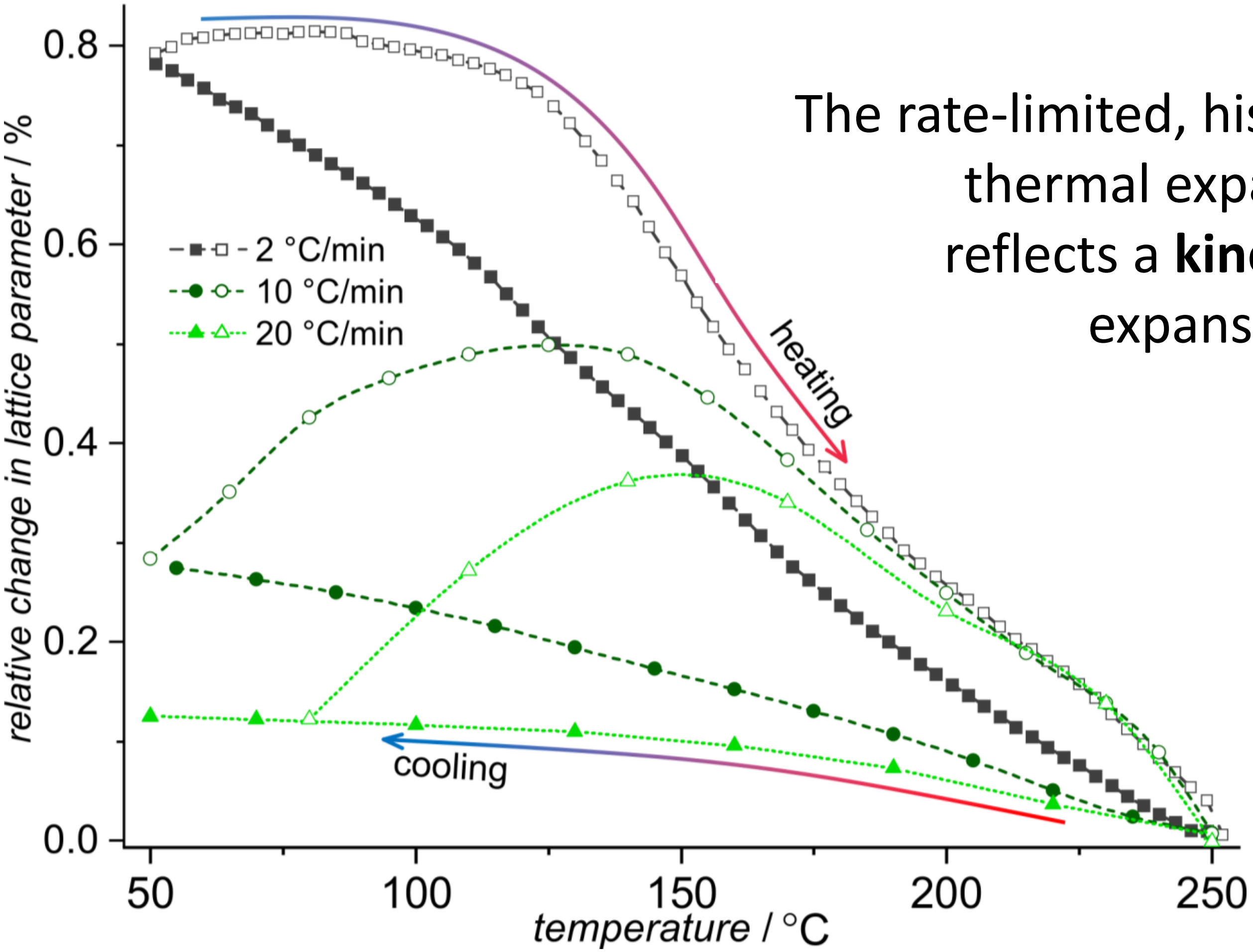

The rate-limited, history-dependent thermal expansion in UiO-66 reflects a **kinetic limitation** in expansion of the lattice with cooling.

Rapid-Actuating Pneumatic Thermal Reactor - RAPTR

The RAPTR quickly heats and cools samples by translating them into and out of a pre-heated hot zone.

So the heating is only limited by the thermal mass of the sample itself

It adapts the resistive heating elements from the original or thermal gradient heater.

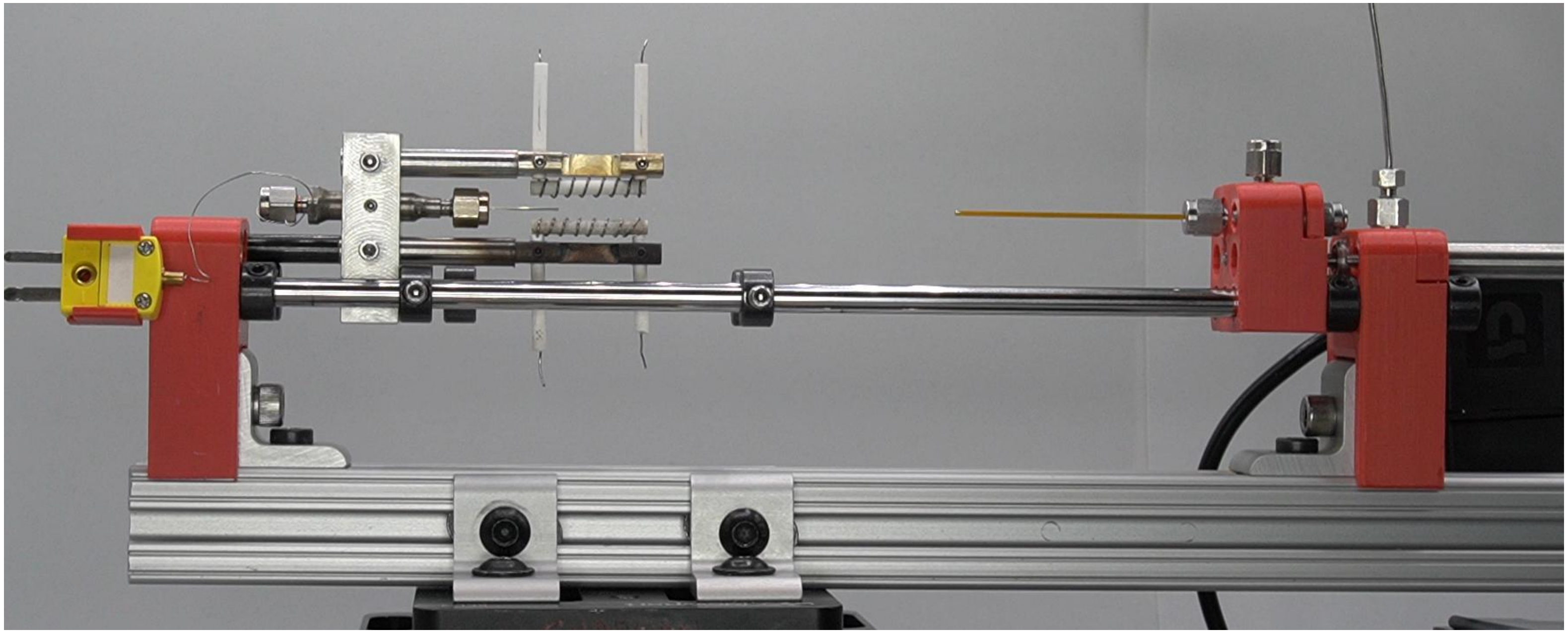

J. Appl. Crystallogr. **2024** 88-93

Fast heating & cooling performance

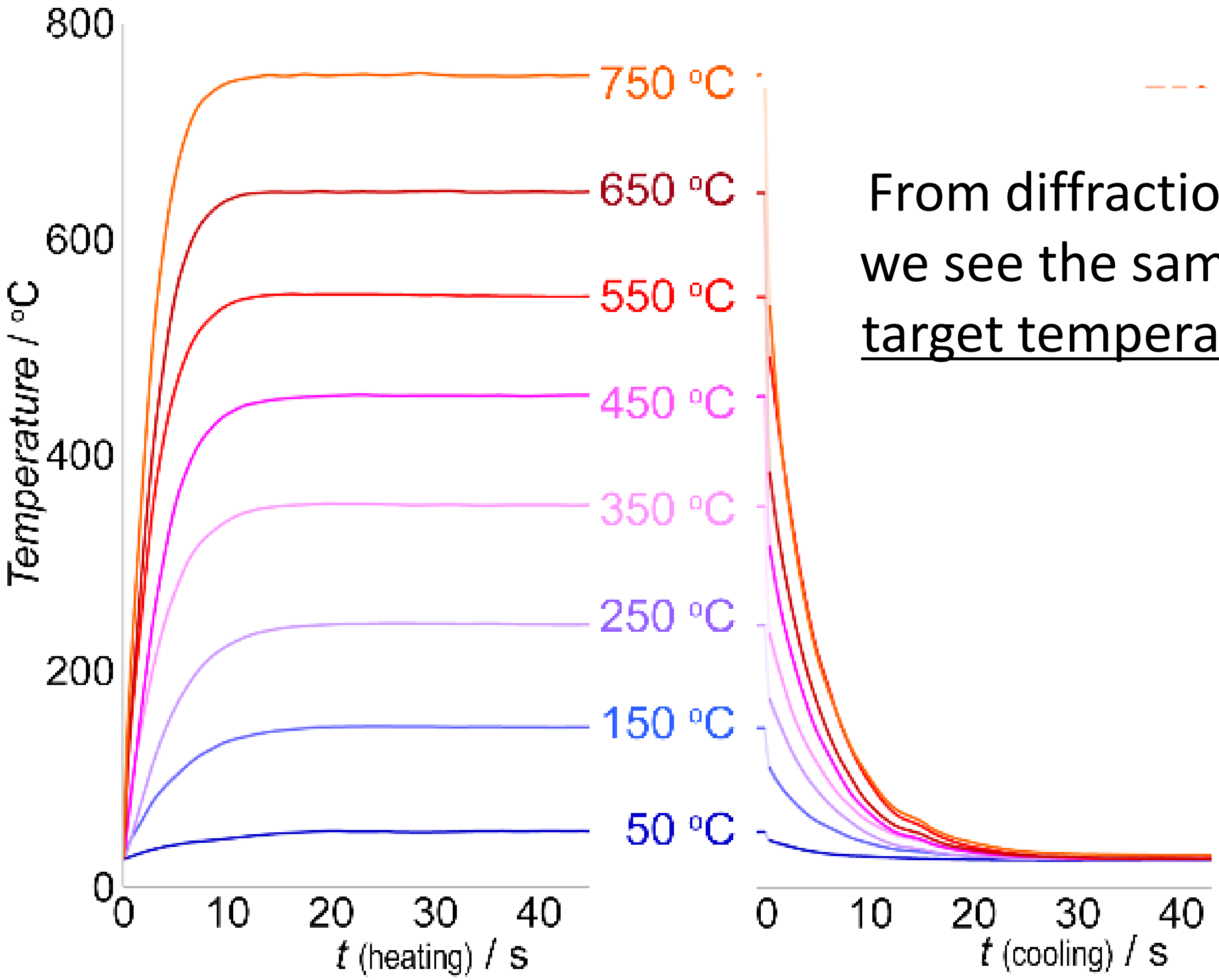

From diffraction thermometry we see the sample reaches the <u>target temperature within 10s</u>.

J. Appl. Crystallogr. **2024** 88-93

J. Am. Chem. Soc. **2024**, 16977

Decoupling time- & temperature-dependence

Use the RAPTR to quantify isothermal relaxation.
Lattice equilibrates faster at high T, but changes more at low T

R apid
A ctuating
P neumatic
T hermal
R eactor

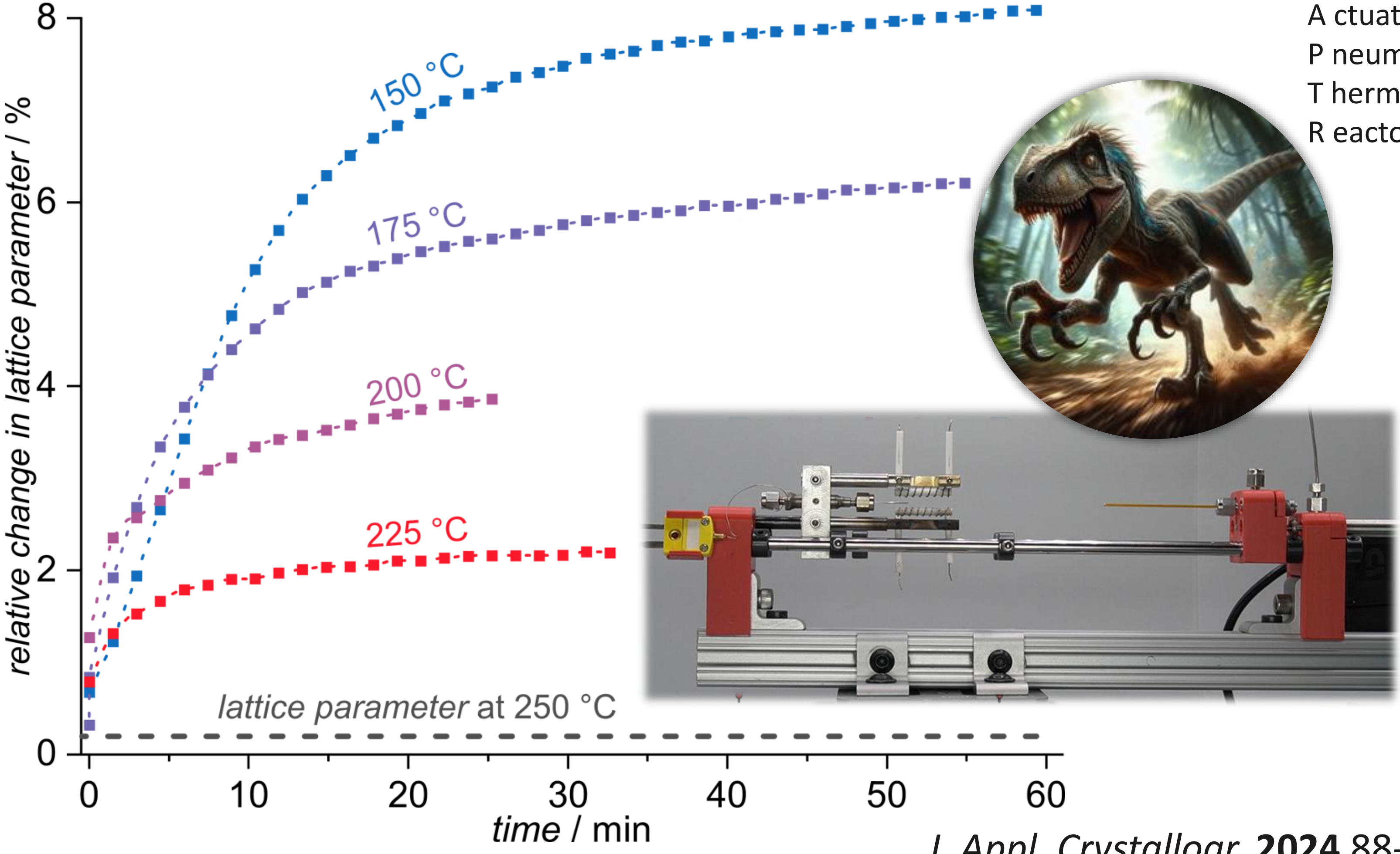

J. Appl. Crystallogr. **2024** 88-93

J. Am. Chem. Soc. **2024**, 16977

Correlation to local node transformation

Rate-dependences and lattice hysteresis is a direct consequence of kinetic trapping of the node-distorted state.

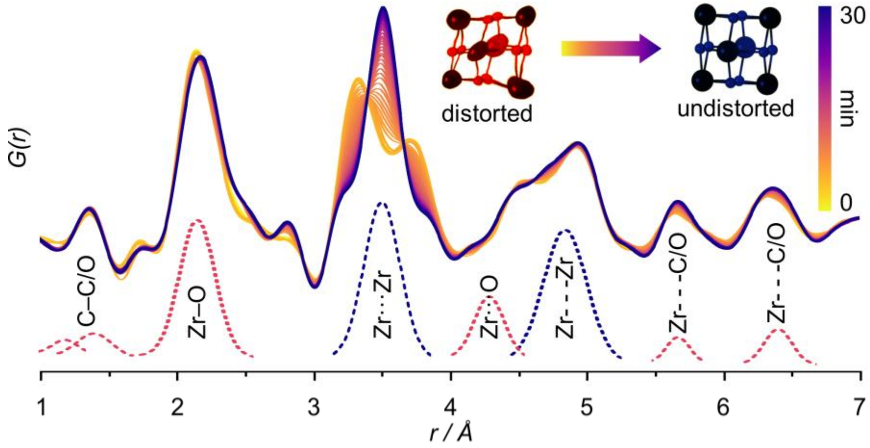

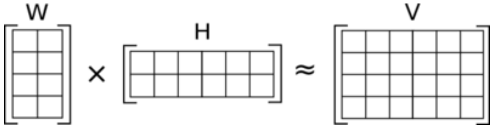

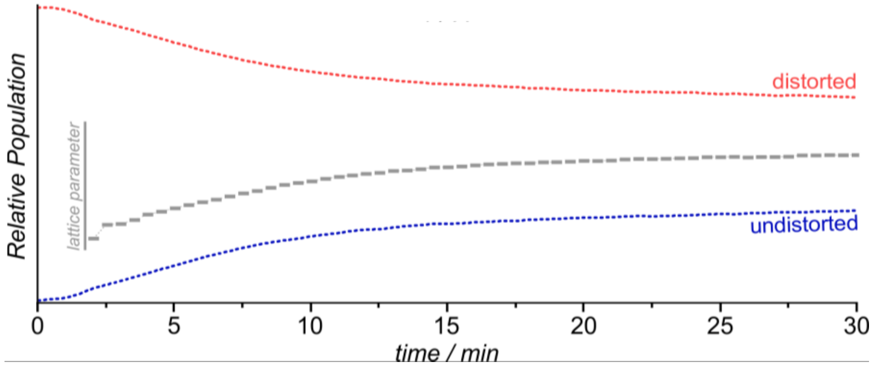

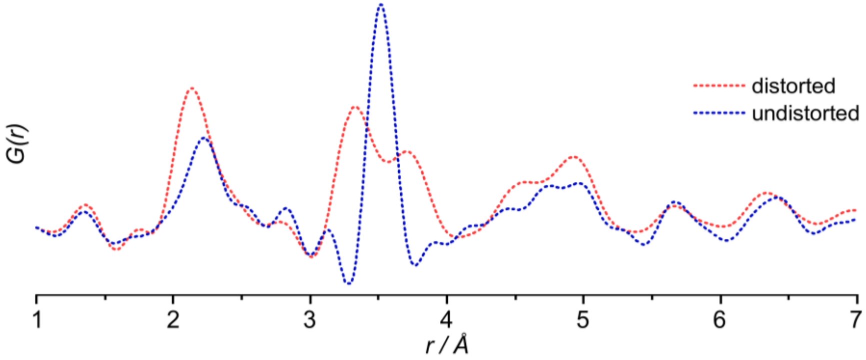

J. Am. Chem. Soc. **2024**, 16977

Node transformation frustrated by framework links

While node distortion is a local phenomenon,
the physical connection between nodes via the organic linker ligand
means that distortion at connected nodes are coupled

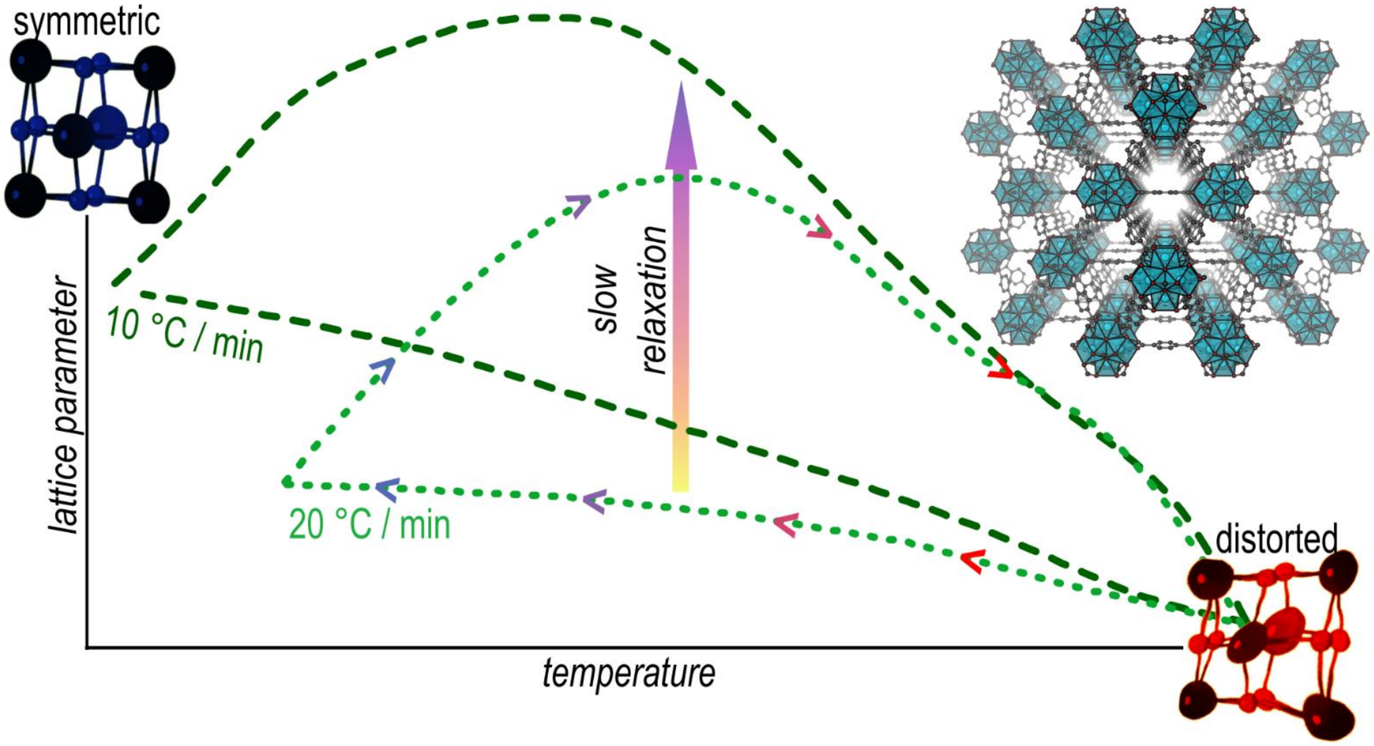

Implications for catalysis and gas capture

Kinetic trapping of the node-distorted state has broad implications for characterizing and applying these of these Zr-MOFs.

The cooling following activation can alter the node and lattice critically impacting gas binding, pore volume, & accessible catalytic sites

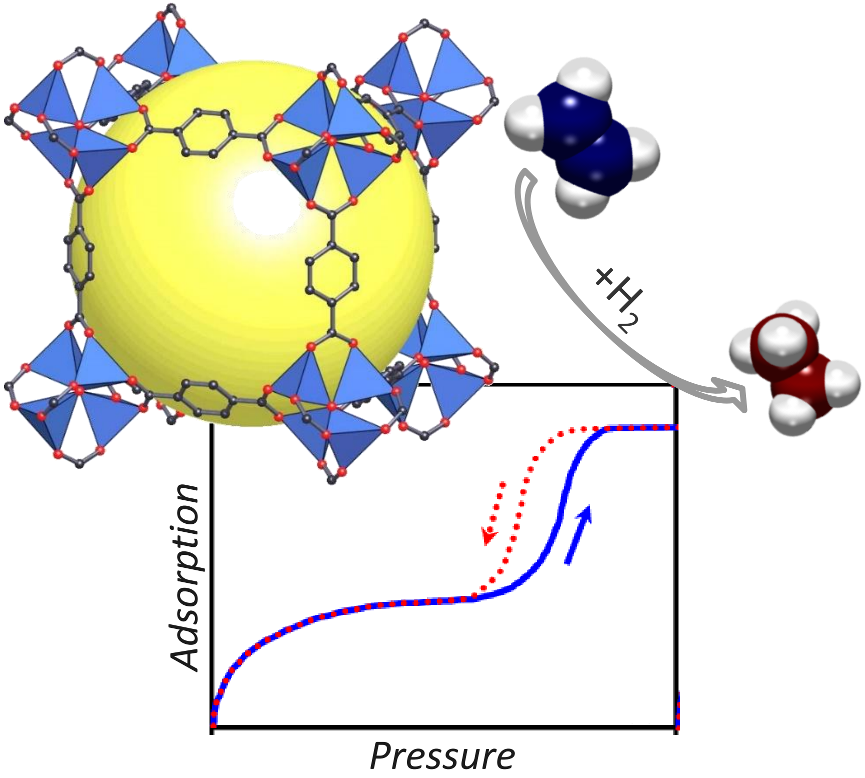

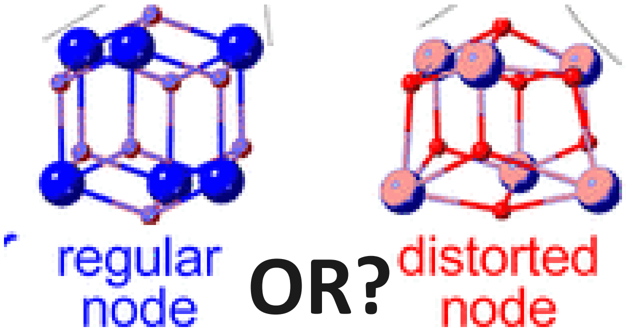

MOFs at the edge of stability

Hypothesis: The node structure and distortions impact nanoparticle formation

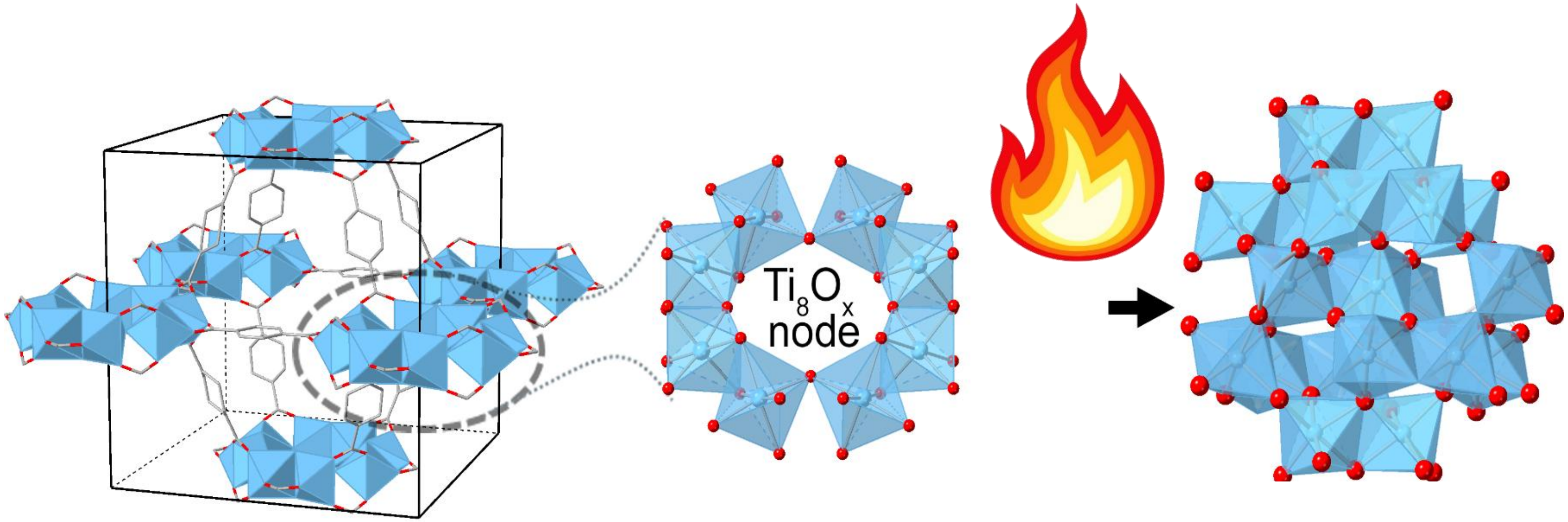

Ti_8 nodes in MIL-125

The cyclic Ti_8 node contains alternating edge- and corner-shared TiO_6 octahedra. These are connected by 12 BDC ligands.

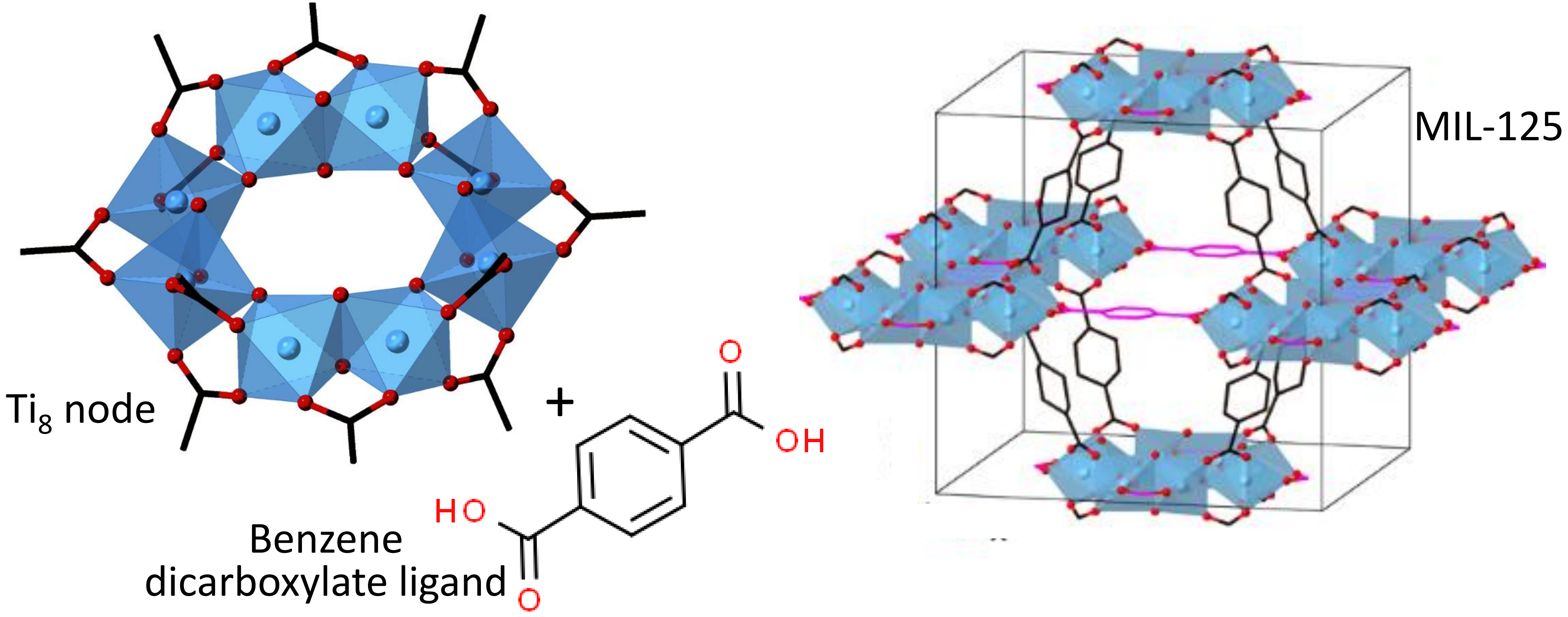

Ferey J. Am. Chem. Soc. 2009, **131**, 10857–10859

Lattice distortion precedes disassembly

Woodrow Chen

The large contraction in the *a*-direction
(& small expansion in *c*-)

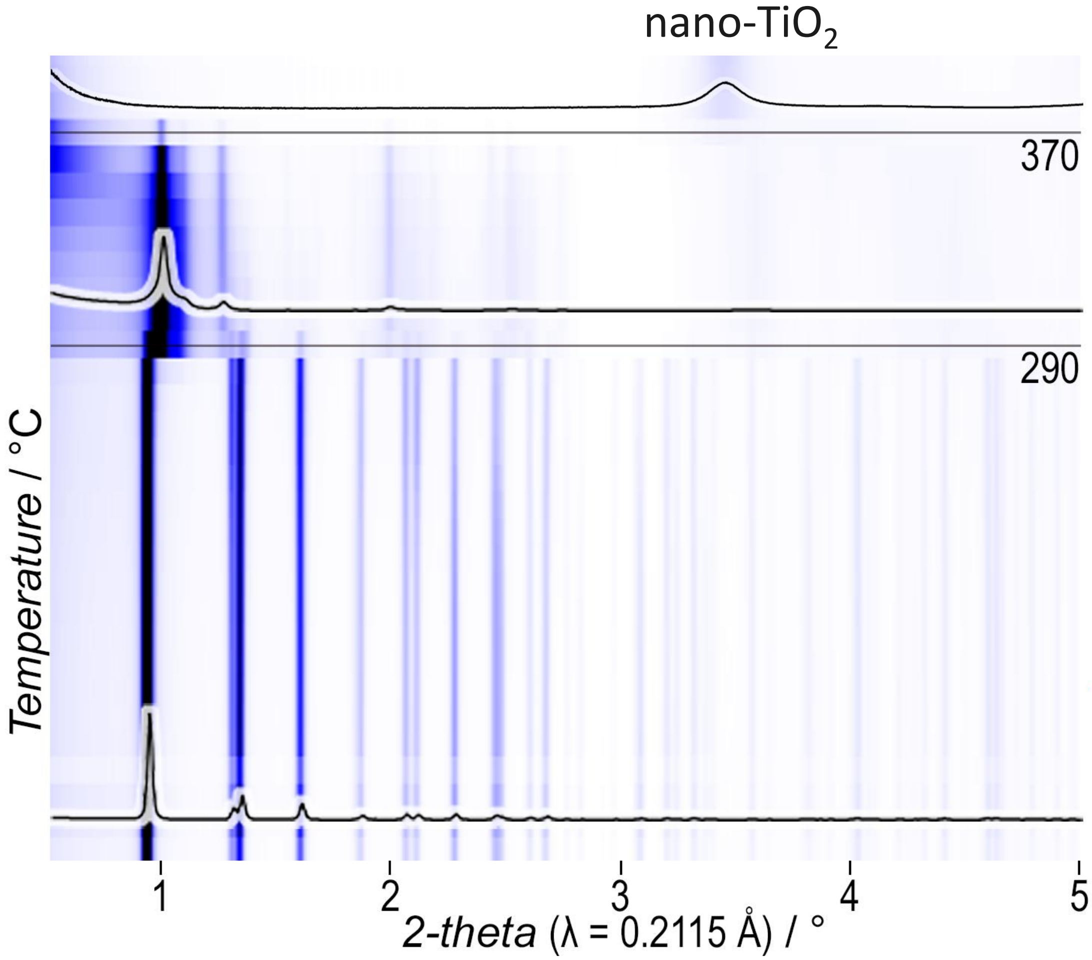

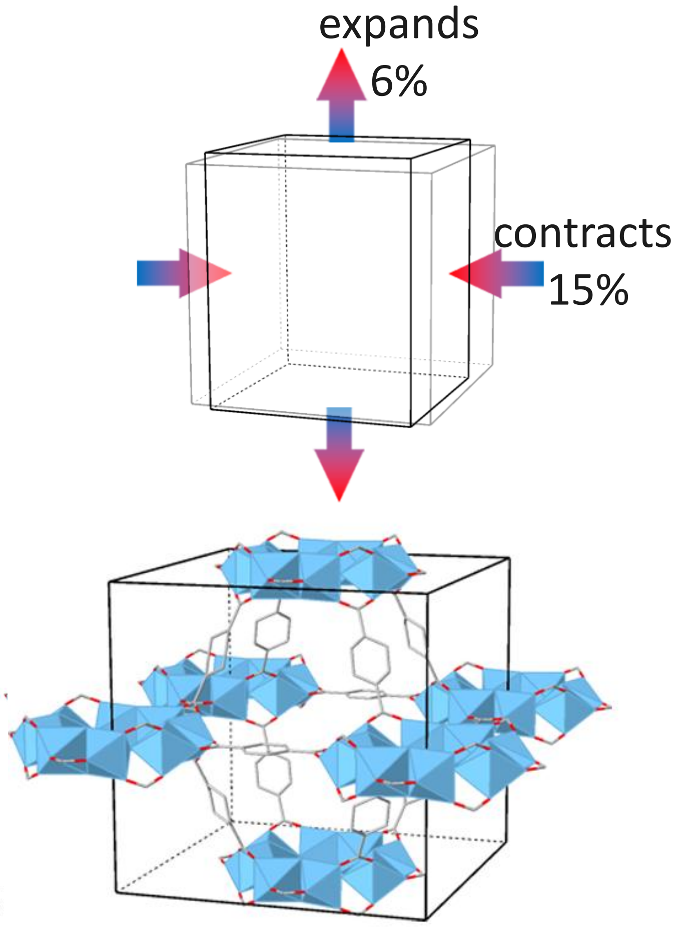

Angew. Chem. ***2025***, *e202501813*

Unusual metastable TiO_2 polymorph observed

Previously, only anatase and rutile have been seen.

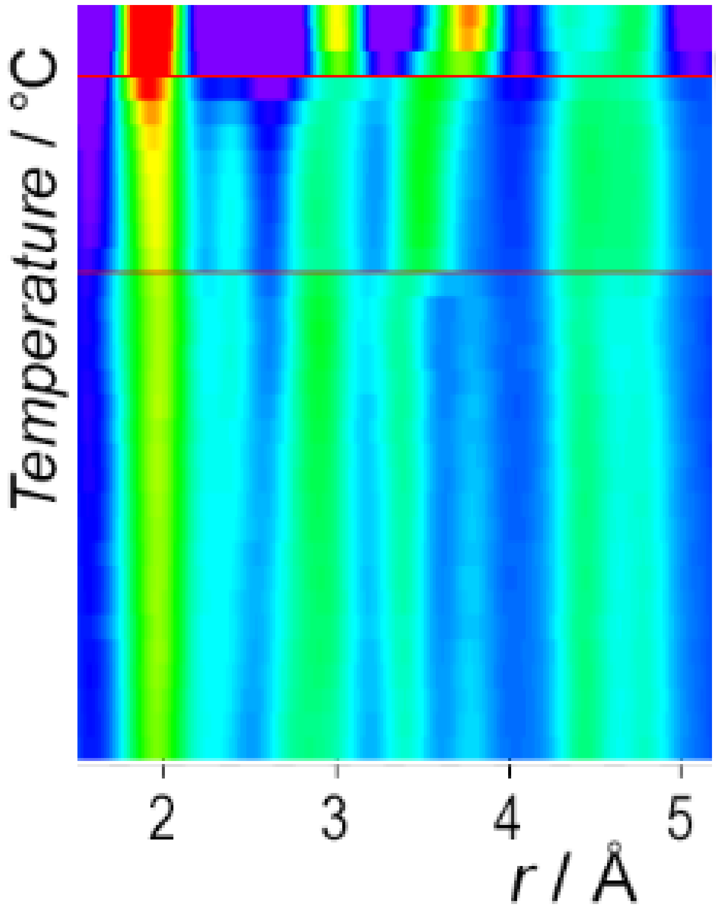

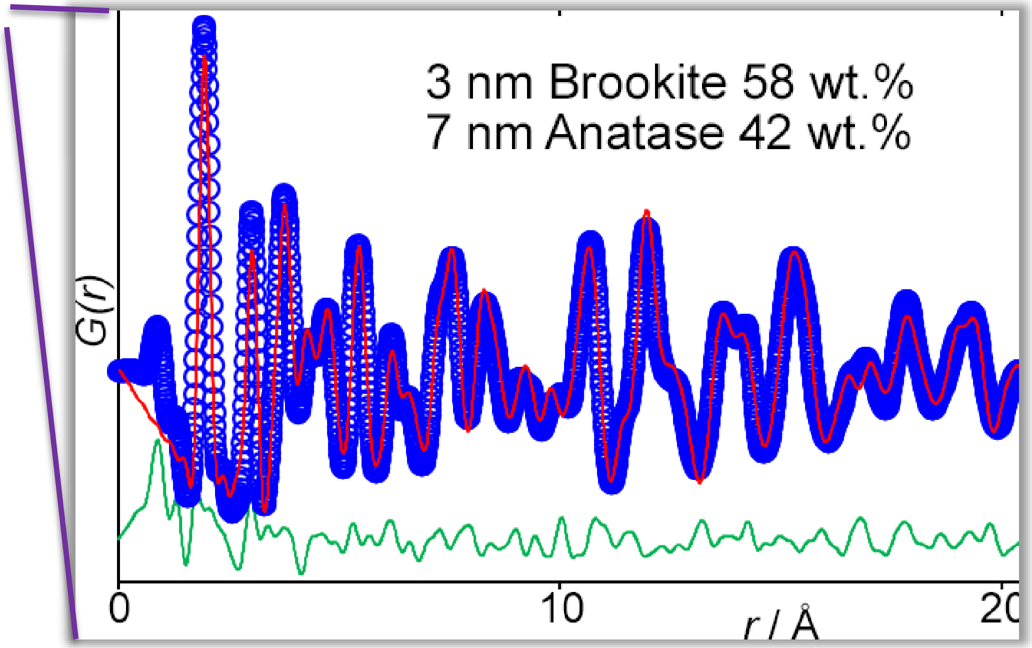

3 nm brookite is unexpected!

Angew. Chem. ***2025***, *e202501813*

TiO_2 is highly polymorphic

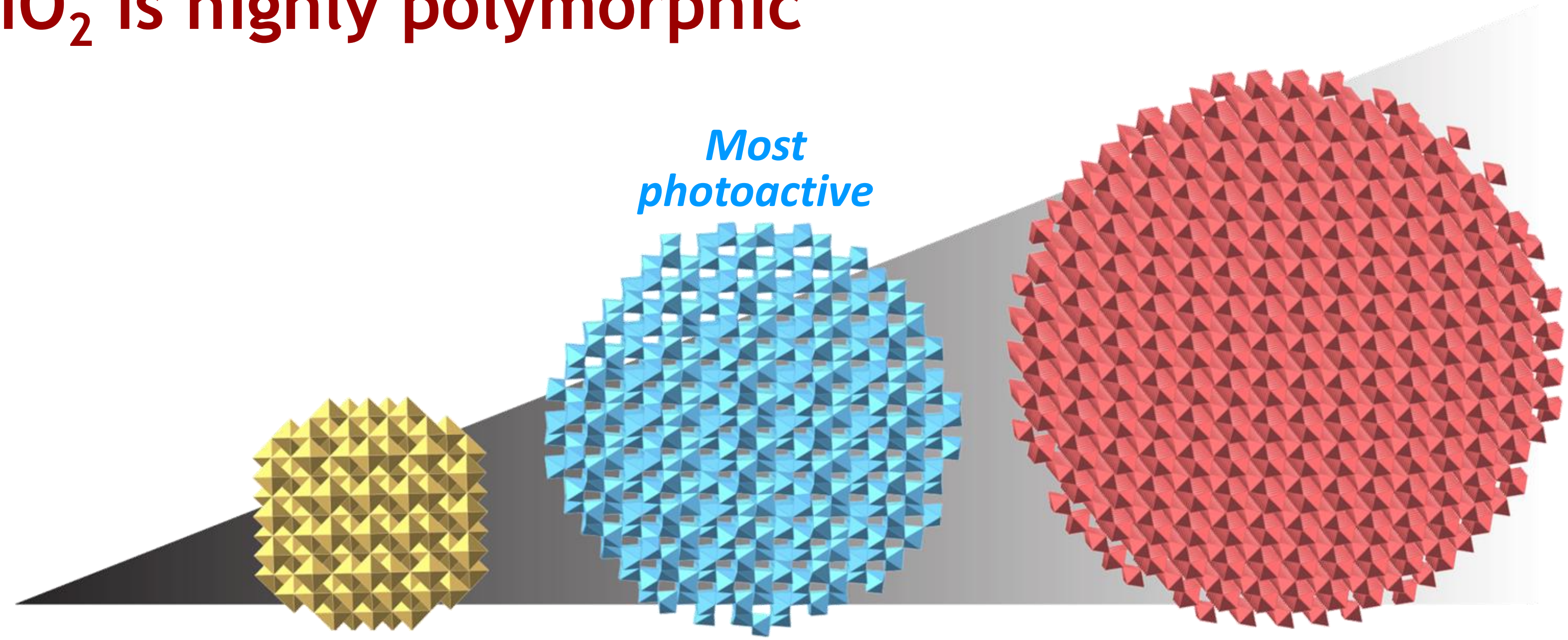

Most photoactive

Anatase
(Metastable)

Brookite
(Metastable)

Rutile

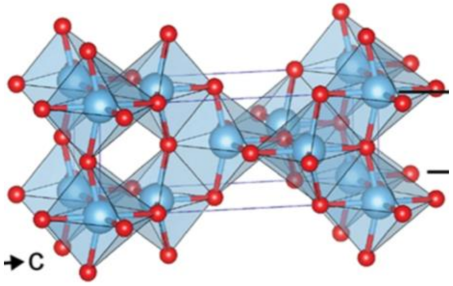

4 edge sharing
4 corner sharing
(all straight)

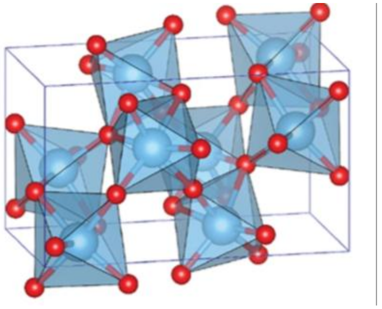

3 edge sharing
6 corner sharing
(4 bent, 2 straight)

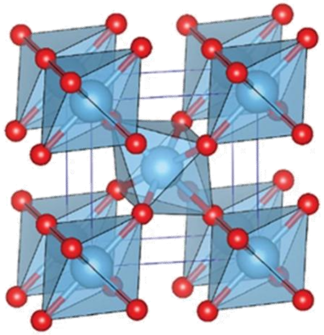

2 edge sharing
8 corner sharing
(all bent)

Ti_8 node distorts

Change from equal number of edge- and corner-shared TiO_6 (like anatase) to more corner-shared TiO_6 (like brookite)

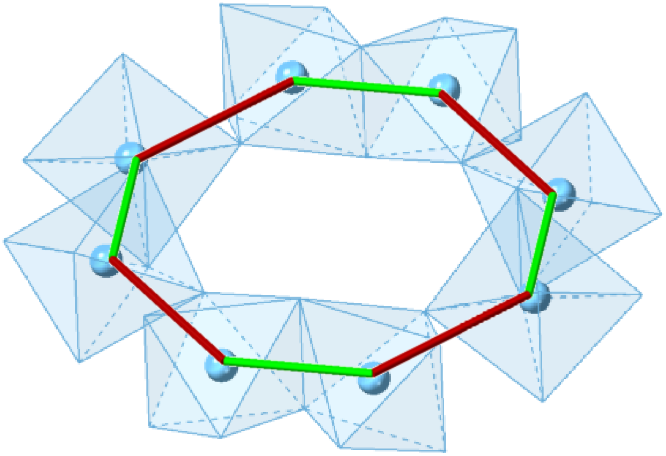

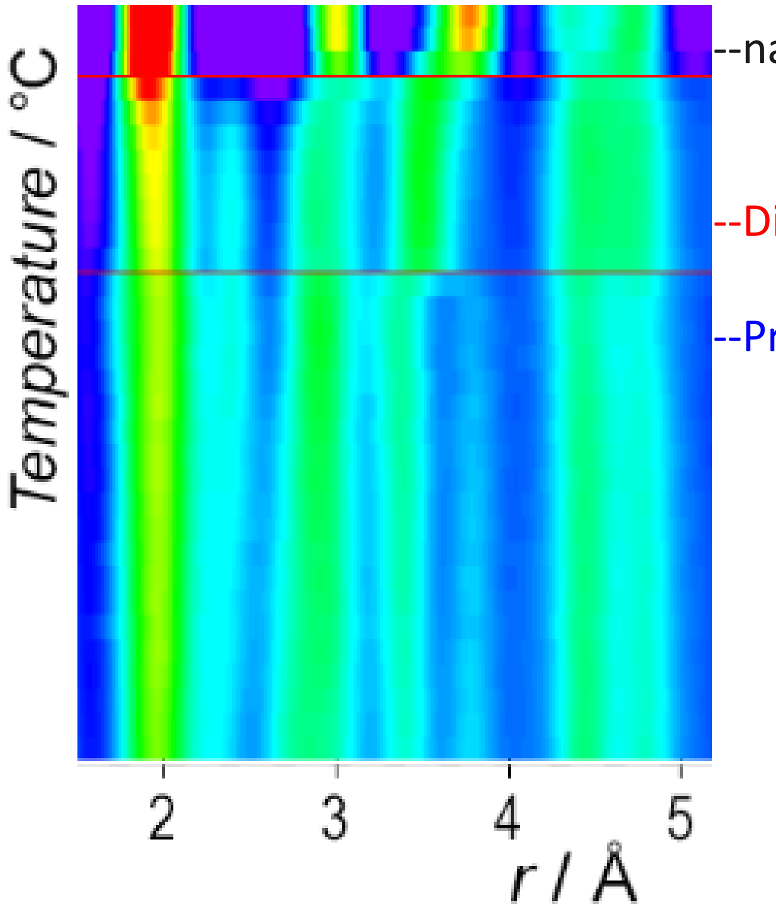

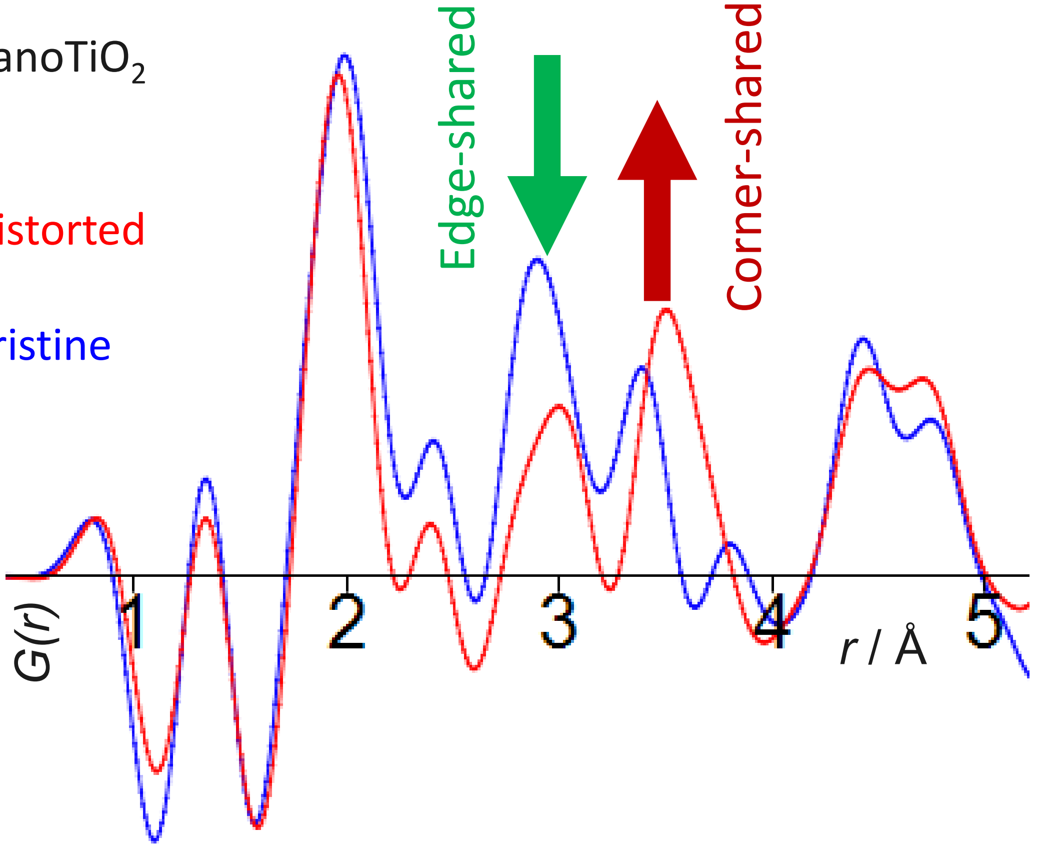

Angew. Chem. **2025**, e202501813

Distorted Ti_8 node resembles brookite polymorph

The structure of the distorted node matches the local structure of the metastable polymorph formed when the MOF destabilizes

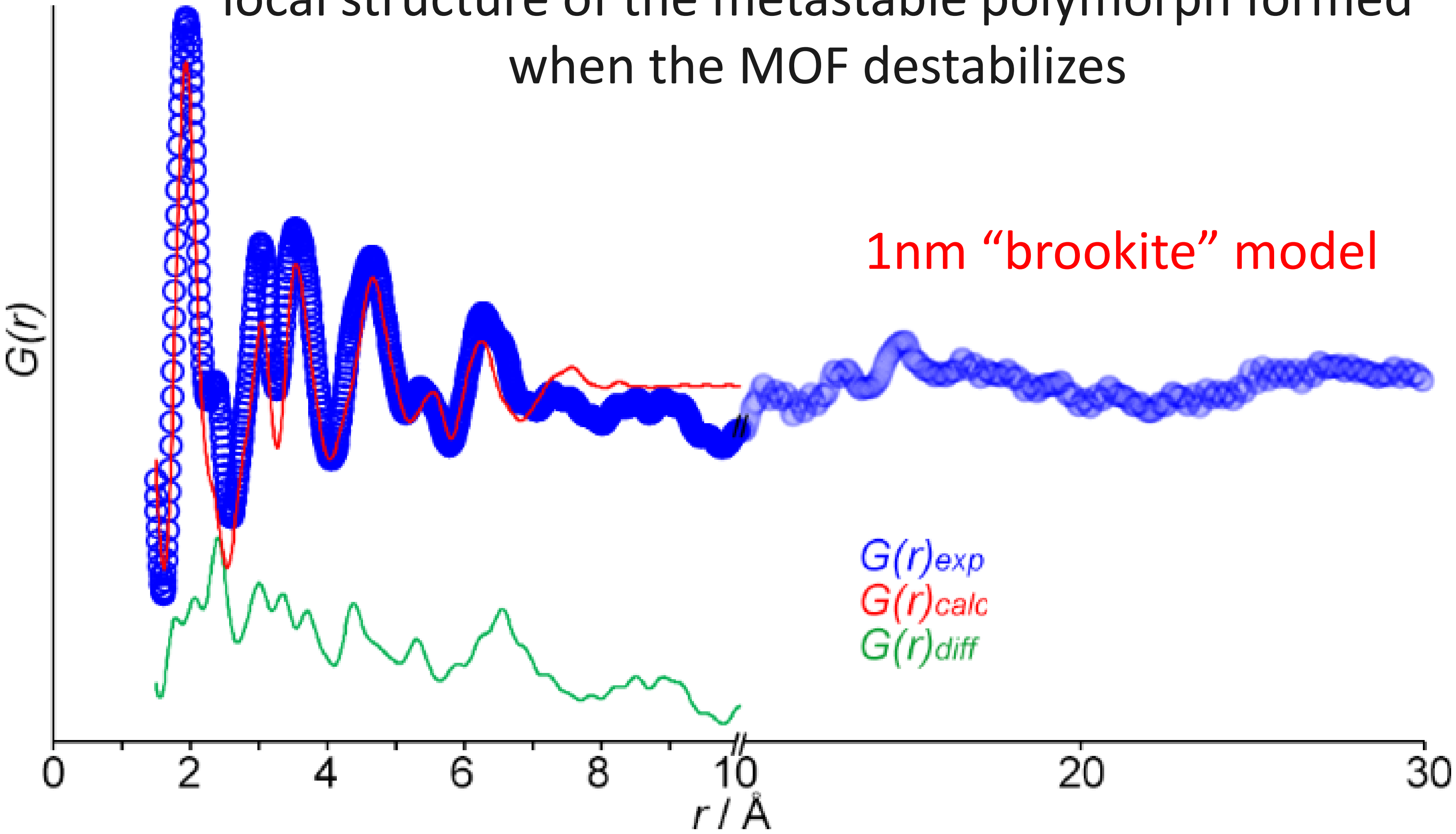

Angew. Chem. ***2025***, *e202501813*

Atmosphere enhances distortion AND brookite

Changing to inert atmosphere shifts
MOF decomposition
to higher T, favors a more complete distortion
and increases brookite product.

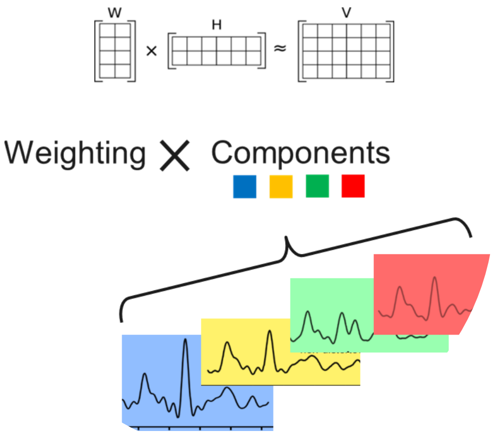

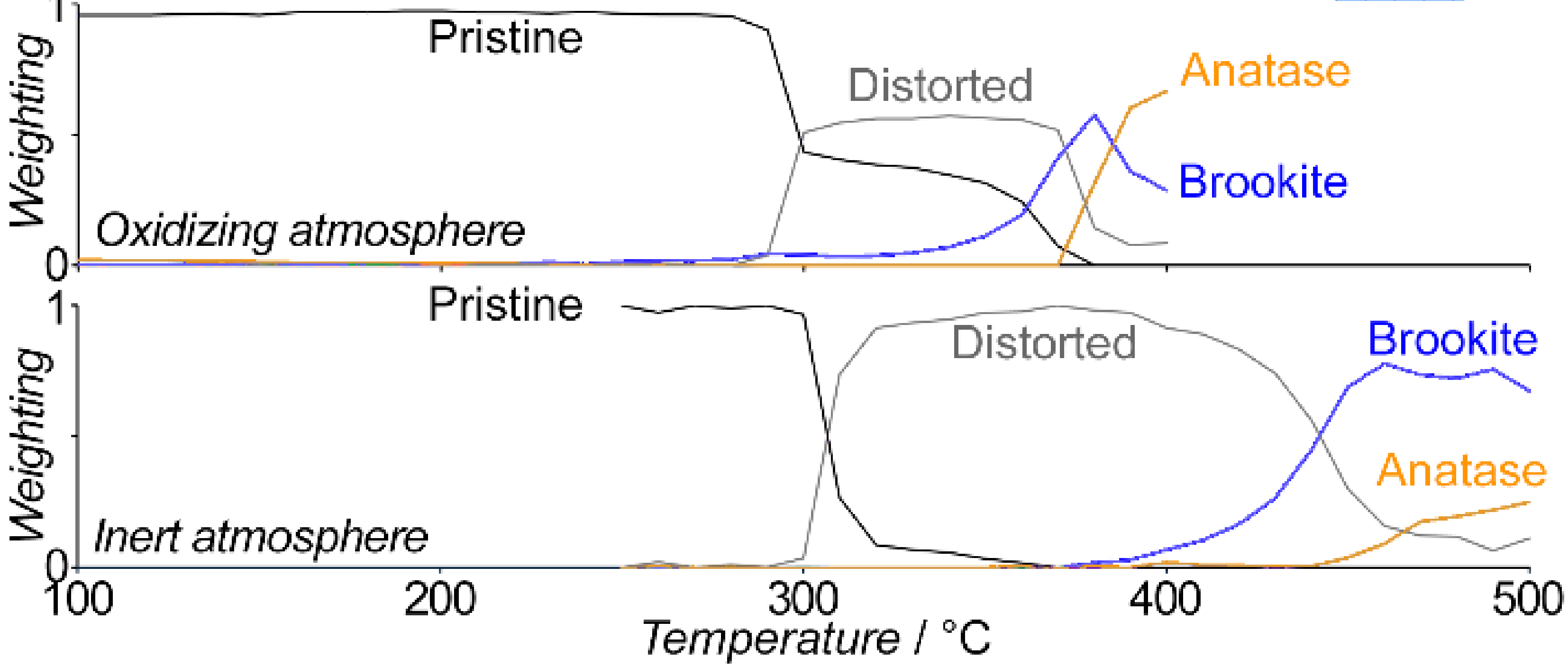

Angew. Chem. ***2025***, *e202501813*

MOFs at the edge of stability

MOFs can serve as unconventional precursors for nanoparticles.

The preorganization of species within the metal-oxo nodes can guide the transformation to unusual nanoparticle polymorphs under mild conditions

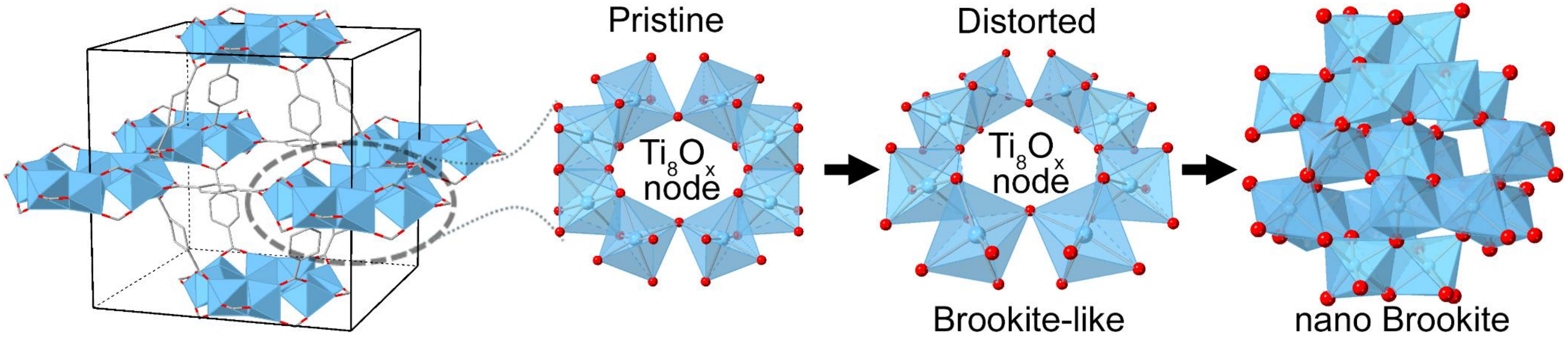

Angew. Chem. ***2025***, *e202501813*

Modern in situ PDF measurements

Modern X-ray Pair Distribution Function measurements

A specialized synchrotron powder diffraction experiment

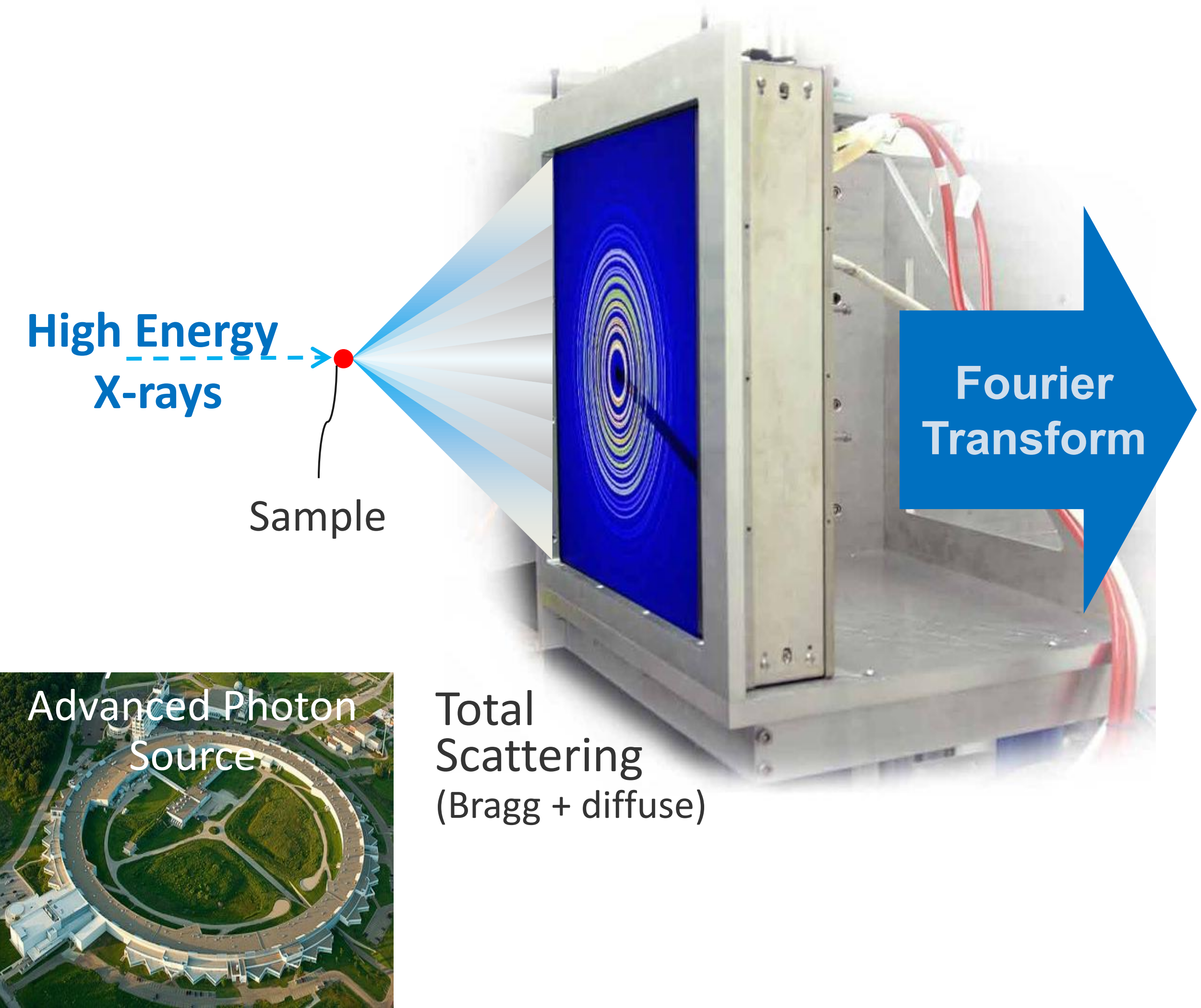

High Energy X-rays

Sample

Fourier Transform

Advanced Photon Source

Total Scattering
(Bragg + diffuse)

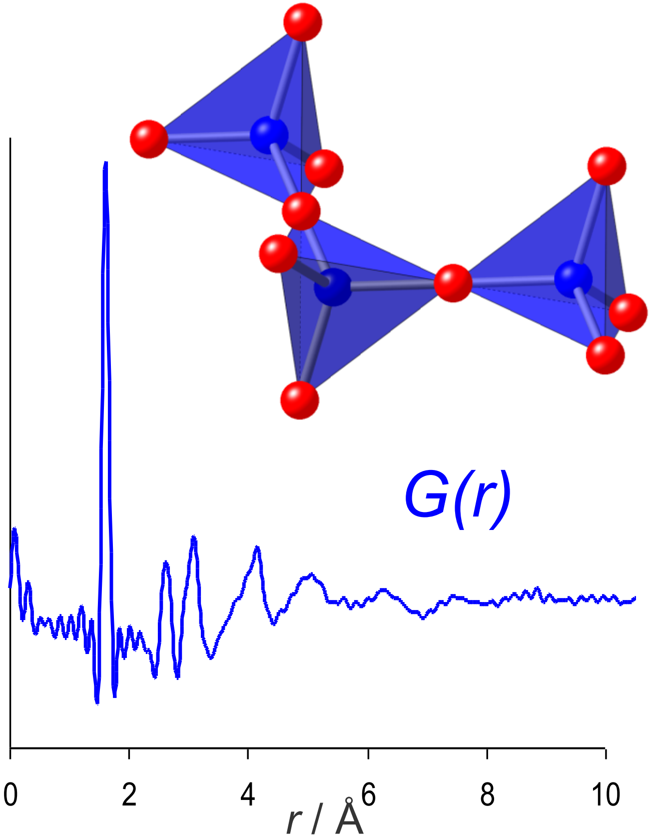

A primer on integrating area detectors

Amorphous Si-based area detectors such as the Varex/PerkinElmer can measure up to 64,000 counts per pixel.

This includes the *sample scattering* and *a dark baseline signal* originating from detector electronics.

Multiple detector read outs are summed to improve signal-to-noise

Limited dynamic range of area detectors

Bryan Sanchez Monserrate

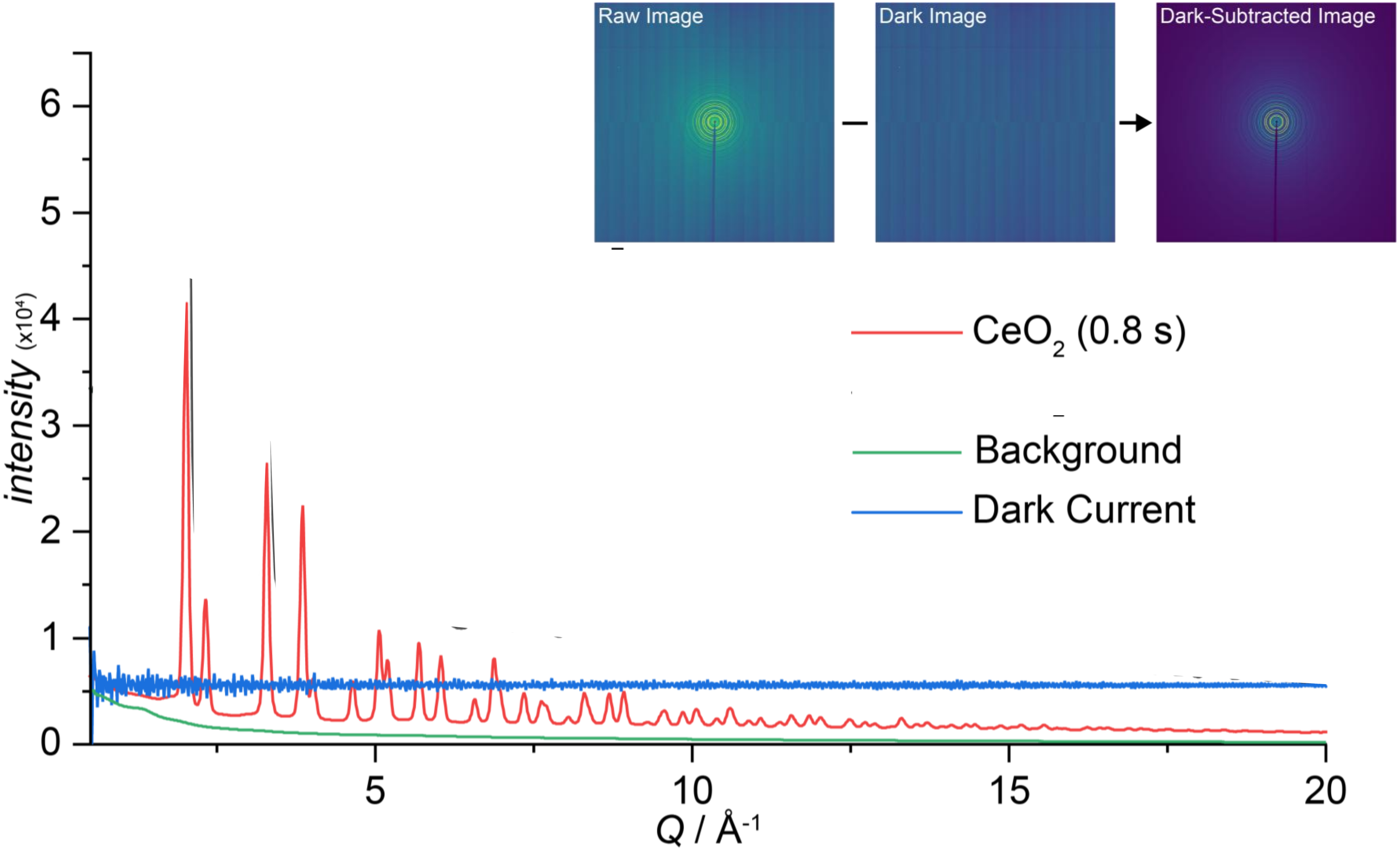

Limited dynamic range of area detectors

Intensities above 64,000 counts are truncated

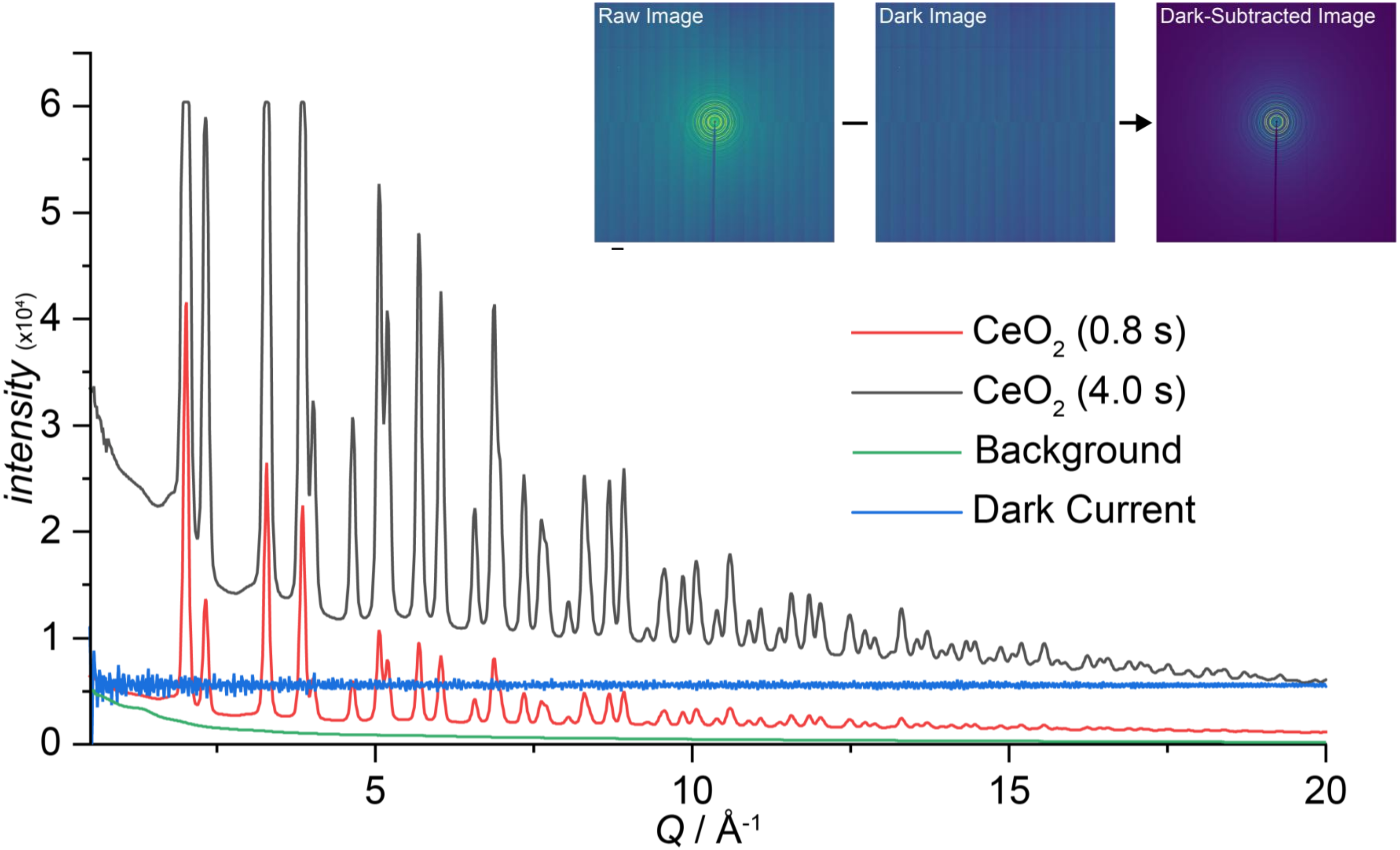

Noise in the image is amplified in *S*(*Q*)/*G*(*r*)

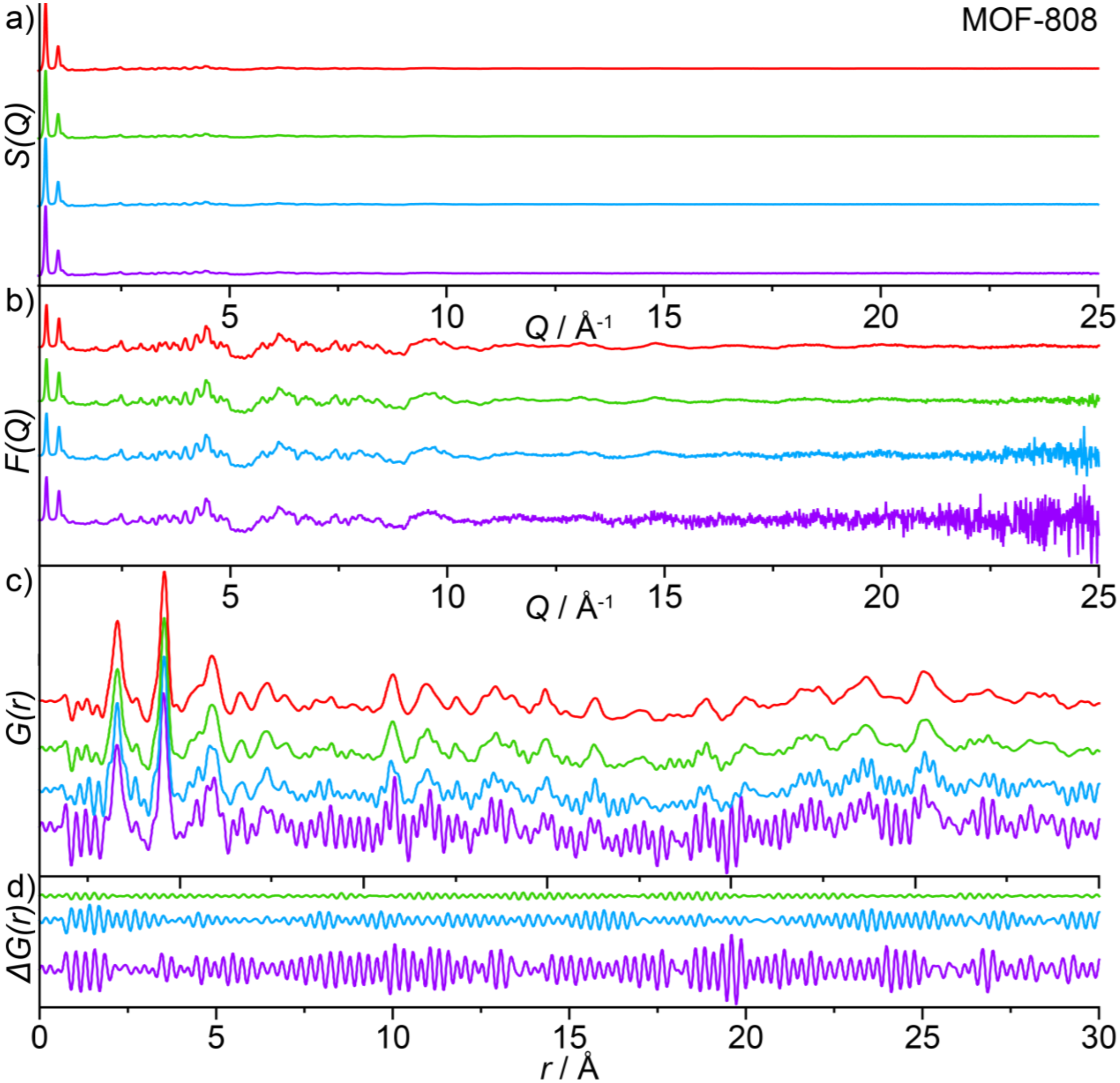

Multiplying by *Q* amplifies noise at high *Q*

Peaks may become overexposed during *in situ* study

E.g. during crystallization

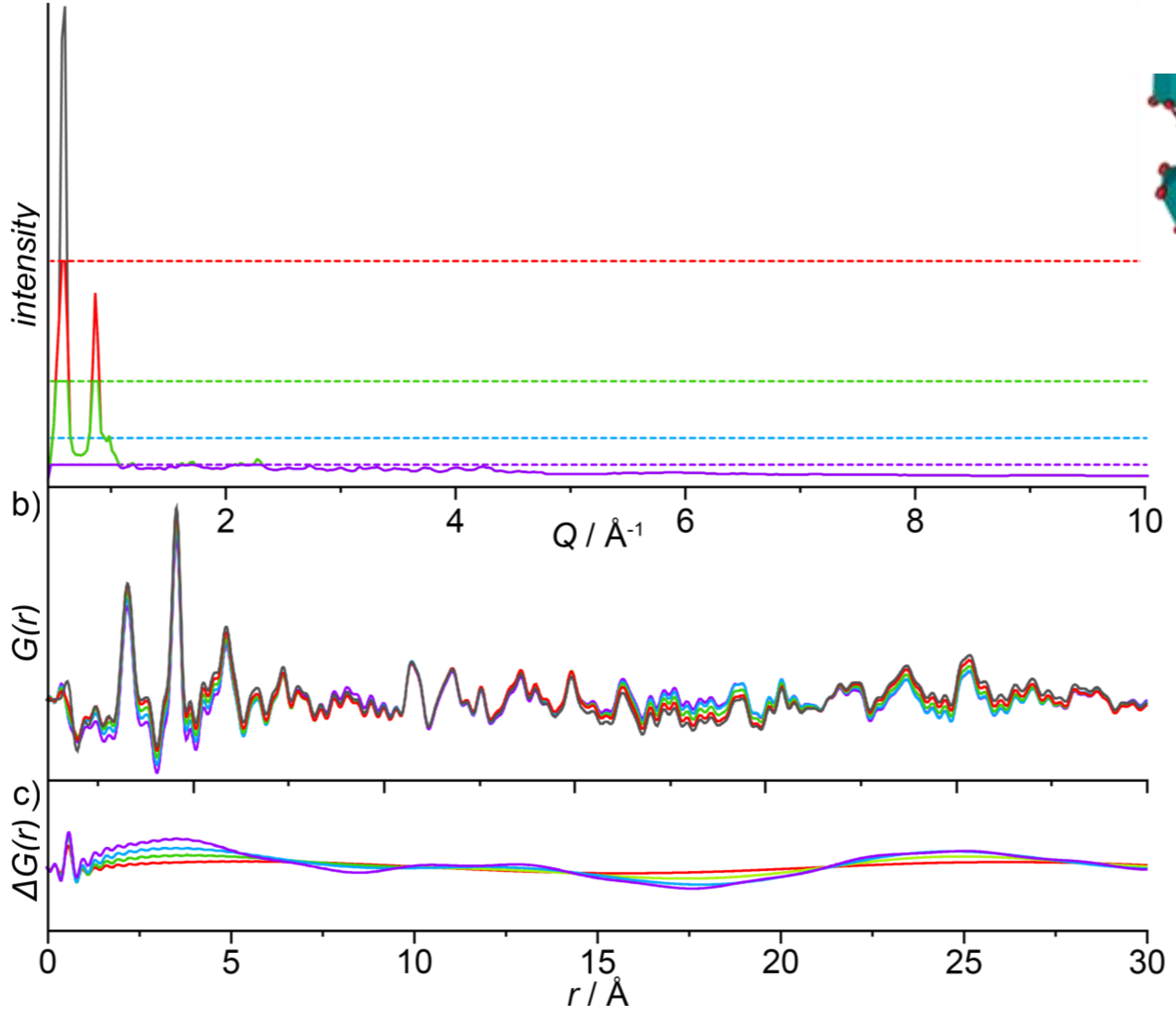

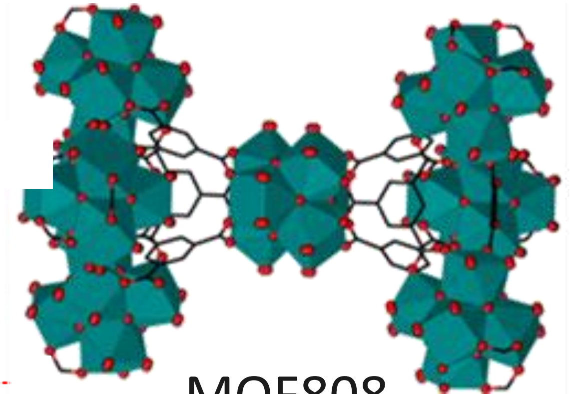

MOF808

Error from truncating peak intensities

Lose porosity features

Peaks may become overexposed during *in situ* study

E.g. during crystallization

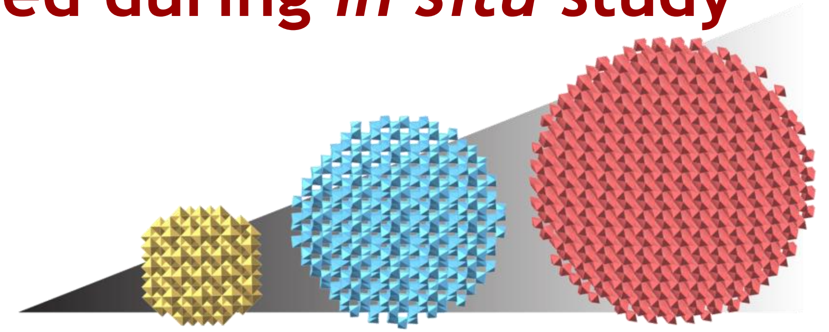

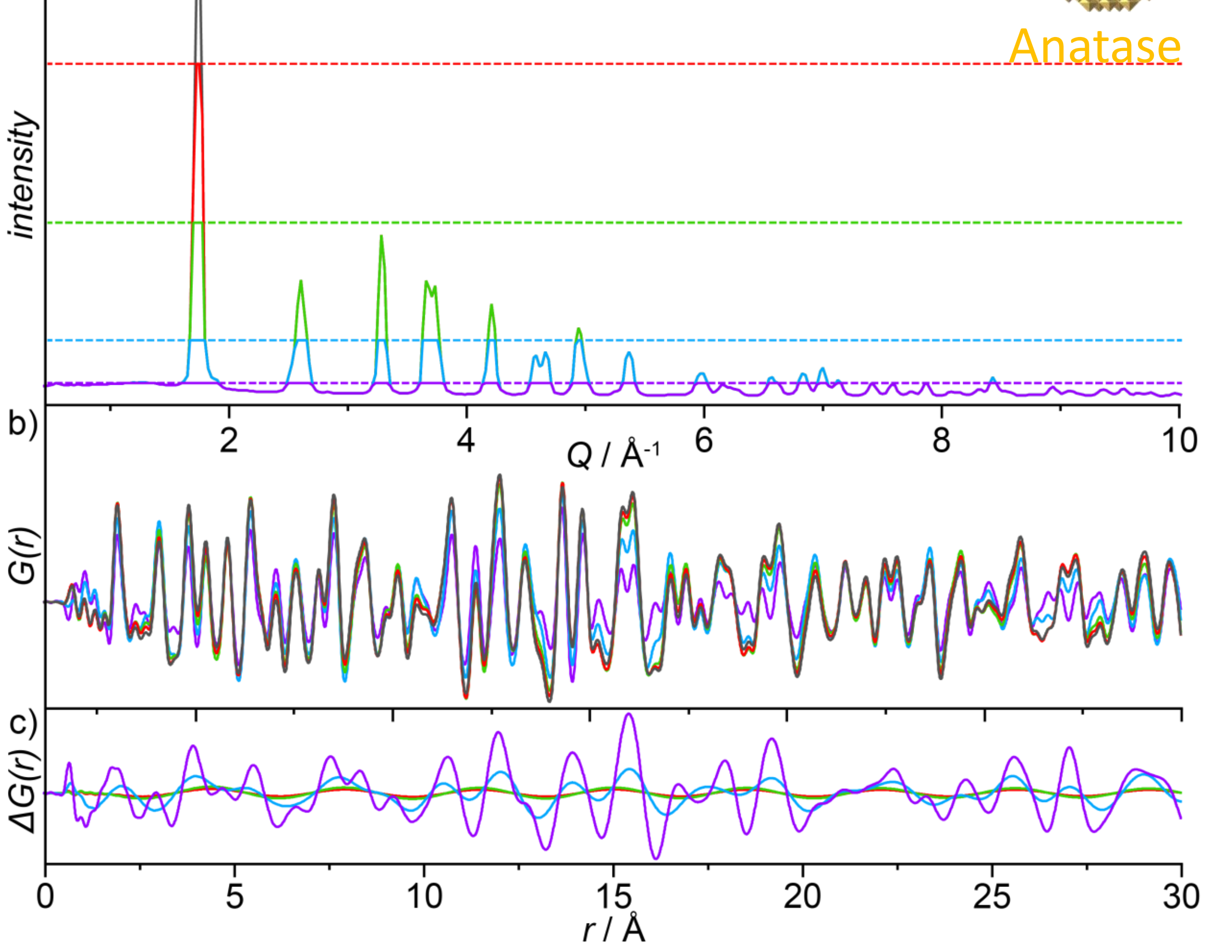

Error from truncating peak intensities

Restoring over-exposed experimental data

Scaling & merging data: Substitute truncated intensity data by intensity data from a less exposed image, for which all the data remain on-scale

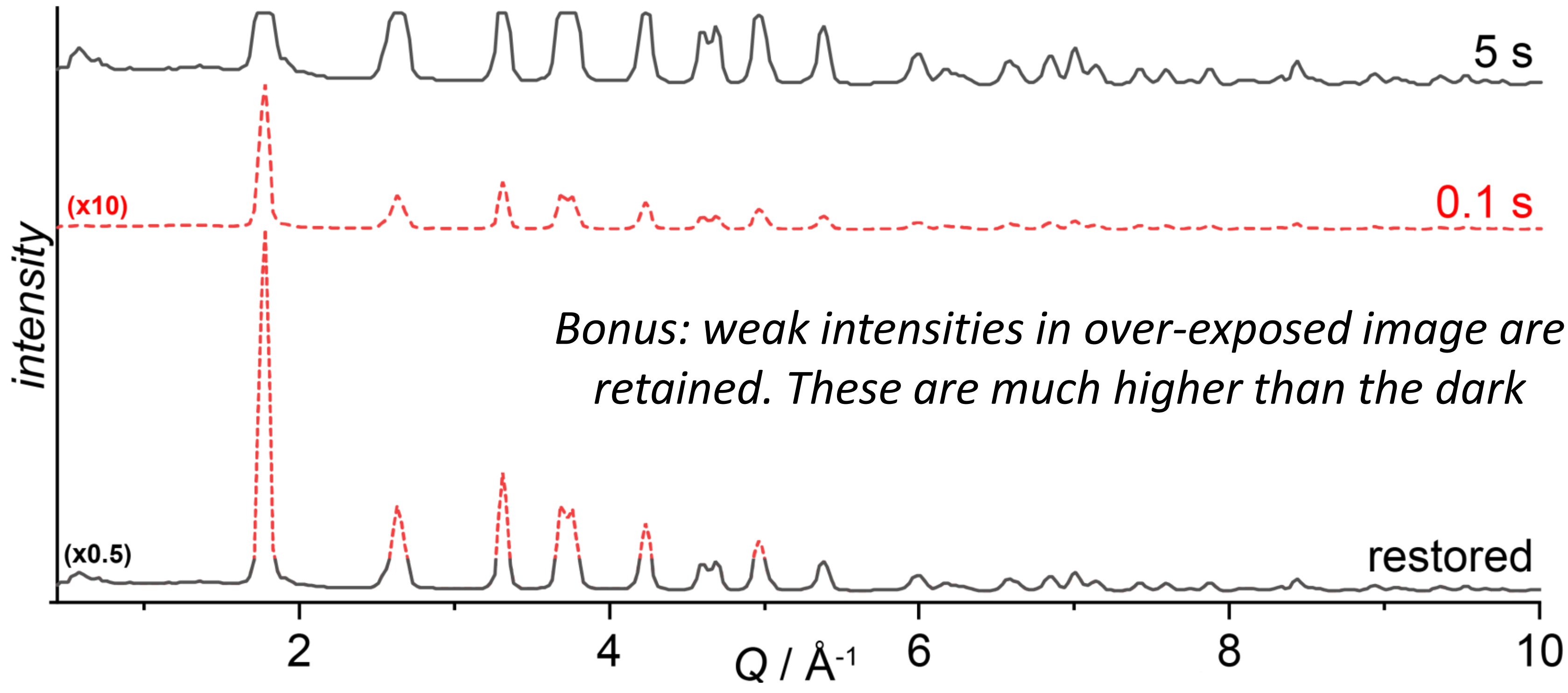

Bonus: weak intensities in over-exposed image are retained. These are much higher than the dark

Patched PDF data are better!

The gain in signal-to-noise ratio of the patched data lead to a lower *r*-factor for same effective exposure time

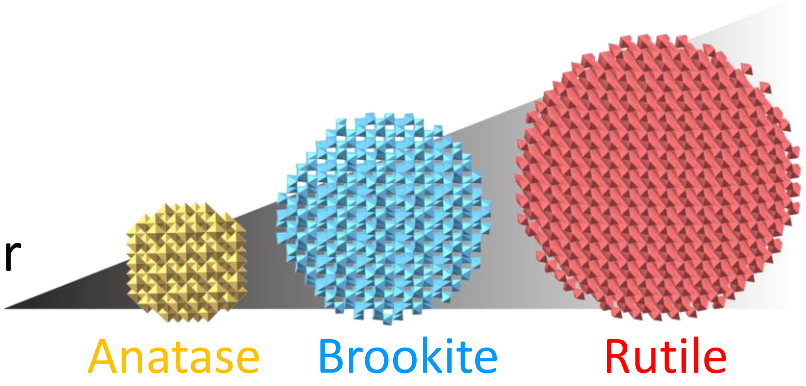

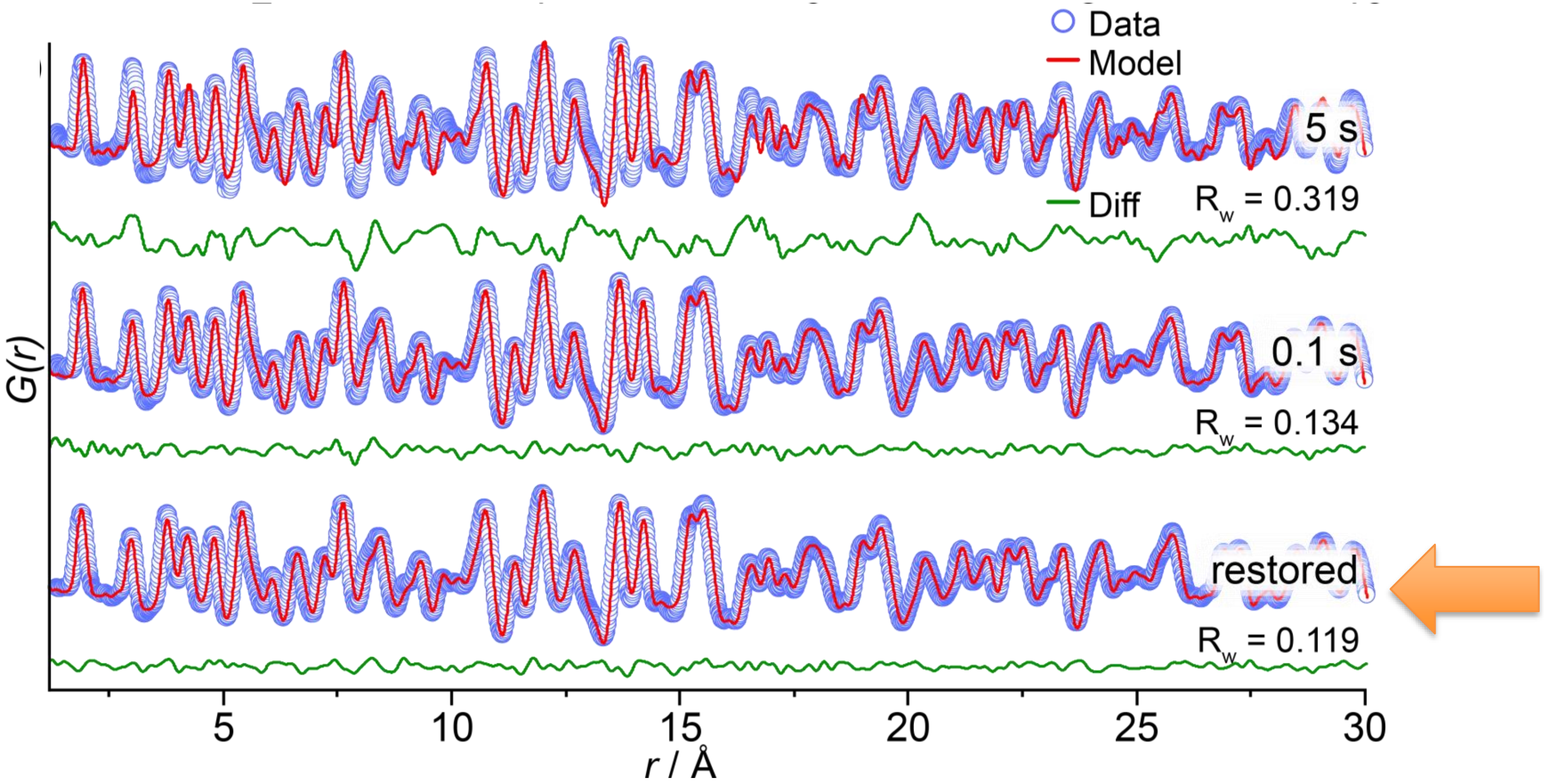

Patched PDF data are better!

Propose this as a *deliberate strategy* for detailed (e.g. RMC) analysis, or weakly scattering/porous systems

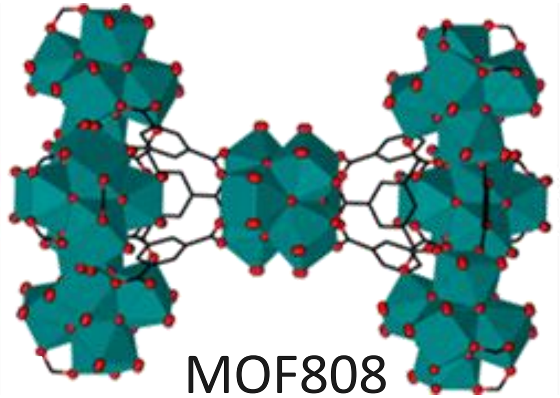

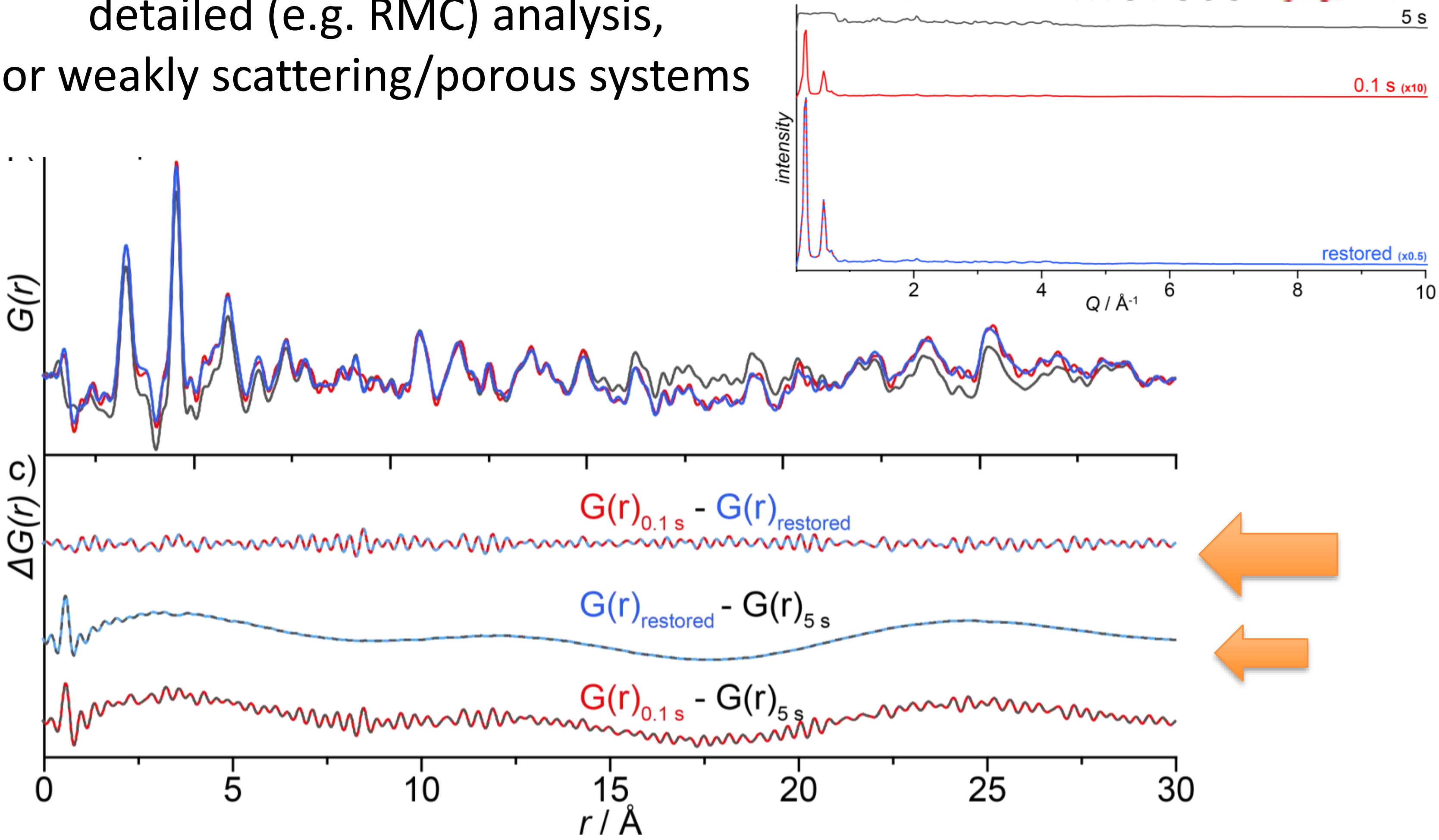

Summary

In situ / operando studies allow you to derive mechanistic insights from individual features, e.g. bondlengths, in the data. Independent of complex structural modeling

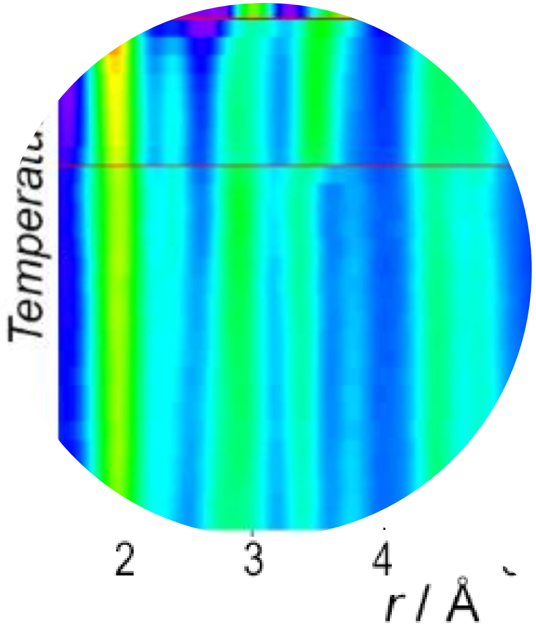

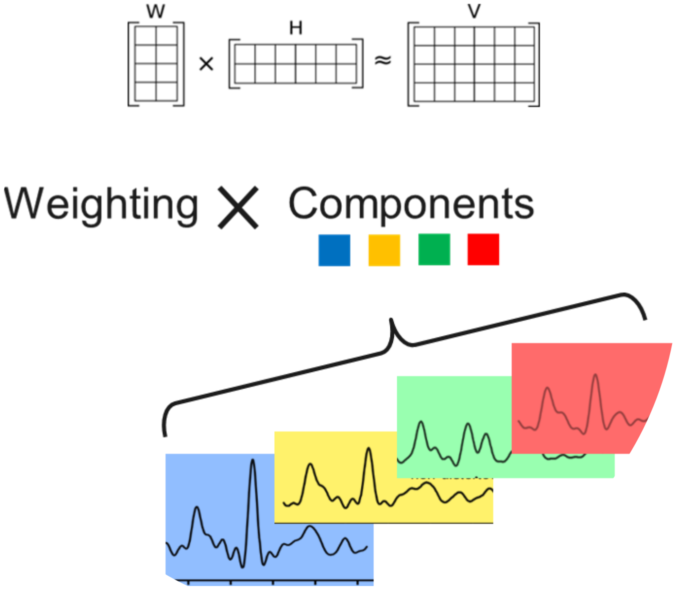

Mutivariate data analytics such as NMF & PCA are powerful tools to help simplify and interpret the interpretation of large volumes of in situ data

Summary

Designing *new in situ reactors and operando sample environments* can be critical to enable materials to be probe under relevant reaction/operating conditions and timescales

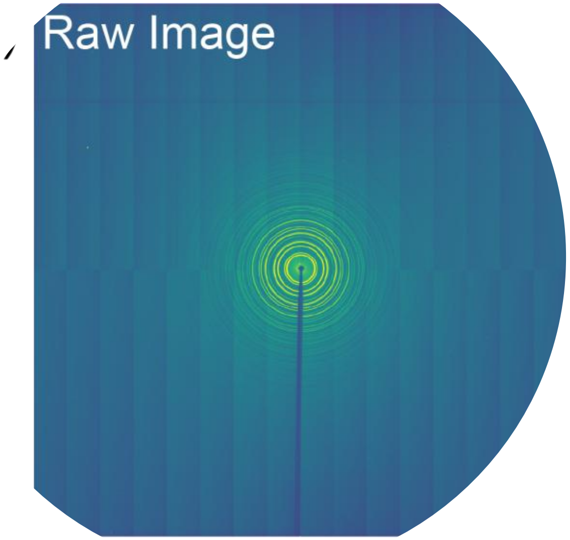

Sometimes, *making mistakes and breaking the rules* can lead to a better way to do measurements

CATALYST DESIGN FOR DECARBONIZATION CENTER
CD4DC

A NEXT **GEN**ERATION
SYNTH**ESIS** CENTER

U.S. DEPARTMENT OF
ENERGY
Office of Science


Fernando Uribe-Romo


Omar Farha


Joe Hupp

Stony Brook University

Use of the Advanced Photon Source, an Office of Science User Facility operated for the U.S. Department of Energy Office of Science by Argonne National Laboratory, were supported by the U.S. Department of Energy under Contract No. DE-AC02-06CH11357.